LOAN DOCUMENT

PHOTOGRAPH THIS SHEET

DTIC ACCESSION NUMBER

LEVEL

INVENTORY 0

AFRL-ML-TY-TR-2001-0041

DOCUMENT IDENTIFICATION

30 MAR 2001

DISTRIBUTION STATEMENT A
Approved for Public Release
Distribution Unlimited

DISTRIBUTION STATEMENT

ACCESSION FOR
NTIS GRA&I ☑
DTIC TRAC ☐
UNANNOUNCED ☐
JUSTIFICATION

BY

DISTRIBUTION/

AVAILABILITY CODES

DISTRIBUTION	AVAILABILITY AND/OR SPECIAL	
A-1		

DISTRIBUTION STAMP

DATE ACCESSIONED

DATE RETURNED

20010711 058

DATE RECEIVED IN DTIC

REGISTERED OR CERTIFIED NUMBER

PHOTOGRAPH THIS SHEET AND RETURN TO DTIC-FDAC

HANDLE WITH CARE

DTIC FORM 70A JUN 90

DOCUMENT PROCESSING SHEET

PREVIOUS EDITIONS MAY BE USED UNTIL STOCK IS EXHAUSTED.

LOAN DOCUMENT

AFRL-ML-TY-TR-2001-0041

Microbial Characteristics of a Reactive Permeable Barrier

Keith A. Strevett and Md. S. Shaheed
Bioenvironmental Engineering & Science laboratory
202 W. Boyd Street, Room #334
Norman OK 73019

AIR FORCE RESEARCH LABORATORY
MATERIALS & MANUFACTURING DIRECTORATE
AIR EXPEDITIONARY FORCES TECHNOLOGIES DIVISION
139 BARNES DRIVE, STE 2
TYNDALL AFB FL 32403-5323

NOTICES

USING GOVERNMENT DRAWINGS, SPECIFICATIONS, OR OTHER DATA INCLUDED IN THIS DOCUMENT FOR ANY PURPOSE OTHER THAN GOVERNMENT PROCUREMENT DOES NOT IN ANY WAY OBLIGATE THE US GOVERNMENT. THE FACT THAT THE GOVERNMENT FORMULATED OR SUPPLIED THE DRAWINGS, SPECIFICATIONS, OR OTHER DATA DOES NOT LICENSE THE HOLDER OR ANY OTHER PERSON OR CORPORATION; OR CONVEY ANY RIGHTS OR PERMISSION TO MANUFACTURE, USE, OR SELL ANY PATENTED INVENTION THAT MAY RELATE TO THEM.

THIS REPORT IS RELEASABLE TO THE NATIONAL TECHNICAL INFORMATION SERVICE
5285 PORT ROYAL RD.
SPRINGFIELD VA 22 161
TELEPHONE 703 487 4650; 703 4874639 (TDD for the hearing-impaired)
E-MAIL orders@ntis.fedworld.gov
WWW http://www.ntis.gov/index.html

AT NTIS, IT WILL BE AVAILABLE TO THE GENERAL PUBLIC, INCLUDING FOREIGN NATIONS.

THIS TECHNICAL REPORT HAS BEEN REVIEWED AND IS APPROVED FOR PUBLICATION.

TIMOTHY G.WILEY, Lt Col, USAF, BSC
Deputy Chief, AEF Tech Division

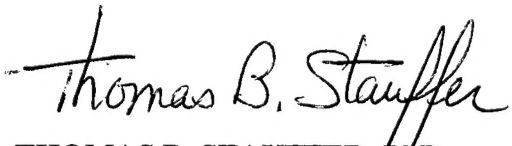

THOMAS B. STAUFFER, PhD
Technical Director, AEF Tech Div

DONALD R. HUCKLE, Jr., Lt Col, USAF
Chief, Air Expeditionary Forces Technologies Division

Do not return copies of this report unless contractual obligations or notice on a specific document requires its return.

REPORT DOCUMENTATION PAGE

Form Approved OMB No. 0704-0188

1. AGENCY USE ONLY *(Leave blank)*	2. REPORT DATE	3. REPORT TYPE AND DATES COVERED
	March 30, 2001	Final August 1998 - February 2000

4. TITLE AND SUBTITLE
Microbial Characteristics of a Reactive Permeable Barrier

5. FUNDING NUMBERS
Subcontract S-4470.4
FO8637-98-C-6002

6. AUTHOR(S)
Keith A. Strevett
Md. S. Shaheed

7. PERFORMING ORGANIZATION NAME(S) AND ADDRESS(ES)
Bioenvironmental Engineering and Science Laboratory
University of Oklahoma
202 West Boyd St., Room 334
Norman, OK 73019

8. PERFORMING ORGANIZATION REPORT NUMBER
Project No.
BEESL-98-990070

9. SPONSORING/MONITORING AGENCY NAME(S) AND ADDRESS(ES)
AFRL/MLQC
139 Barnes Drive, Suite 2
Tyndall AFB, FL 32403-5323

10. SPONSORING/MONITORING AGENCY REPORT NUMBER

11. SUPPLEMENTARY NOTES

12a. DISTRIBUTION AVAILABILITY STATEMENT

12b. DISTRIBUTION CODE

13. ABSTRACT *(Maximum 200 words)*

Permeable reactive barriers for treatment of subsurface organic and inorganic contaminants is recent technology. Little research has been done to its potential problem areas and to measure long-term performance. Observed flow reductions and performance deterioration is typically postulated as a consequence of chemical precipitation. Thus, knowlege about biofouling of these barriers is limited. This study presents a methodology to predict the biofouling potential of permeable reactive barriers through the investigation of dominant microbial groups and using their surface thermodynamic characteristics. Predominant microbial groups were enumerated from soil cores obtained from the permeable barrier at Dover National Test Site, Dover AFB, DE. Hydrophobicity of the microorganisms and their interaction energies with the zero valent iron (ZVI) at different physiological states were quantified. Sulfate reducing bacteria (SRB), anaerobic heterotrophs and aerobic heterotrophs were detected at the site, of which SRB were the dominant group of microorganisms in the ZVI. The Gibbs free energy of SRB cells interaction with ZVI showed highest potential for adhesion at logorithmic state. Predicted observations were confirmed with batch partitioning experiments.

14. SUBJECT TERMS
permeable reactive barrier, biofouling, Gibbs free energy, adhesion, sulfate reducing bacteria

15. NUMBER OF PAGES
38

16. PRICE CODE

17. SECURITY CLASSIFICATION OF REPORT	18. SECURITY CLASSIFICATION OF THIS PAGE	19. SECURITY CLASSIFICATION OF ABSTRACT	20. LIMITATION OF ABSTRACT
Unclassified	Unclassified	Unclassified	UL

PREFACE

This report was prepared by Keith A. Strevett and Md. S. Shaheed, Bioenvironmental Engineering and Science Laboratory, University of Oklahoma, 202 W. Boyd St., Rm.#334, Norman, OK 73019, Subcontract: S-4470.4, under Air Force Prime Contract: F08637-98-C-6002, for Applied Research Associates, Incorporated, 4300 San Mateo Boulevard, NE, Suite A-220, Albuquerque, NM 87110.

This final report describes identification and enumeration of dominant microbial groups up-gradient, within, and down-gradient of an active reactive permeable barrier installed in Dover Air Force Base, Kent County, Delaware; quantification of electrodynamic and electrostatic surface potentials of dominant microbial groups and the reactive core material; and a projective analysis of the surface thermodynamic properties to biofouling potential of the reactive permeable barrier.

The work was performed between May 1999 and May 2000. The AFRL project manager was Ms. Alison Lightner. The authors wish to acknowledge the valuable sampling support received for the Dover National Test site and the project support received from the Strategic Environmental R&D Program (SERDP).

THIS PAGE IS INTENTIONALLY LEFT BLANK

EXECUTIVE SUMMARY

A. OBJECTIVE

The goal of this research is the development and implementation of microbial surface thermodynamic technology that can be used to predict microbial adhesion characteristics and ultimate biofouling. This goal is achieved via identification of dominant microbial groups up-gradient, within and down-gradient of a reactive barrier, enumeration of identified microbial groups, and quantification of electrodynamic and electrostatic surface potentials of dominant microbial groups.

B. BACKGROUND

Subsurface sorptive-reactive treatment zone, which is commonly called a Permeable Reactive Barrier (PRB), is a recent technology for treating various organic (17, 33, 45) and inorganic (3, 6, 19) contaminants. PRBs offer an economic alternative over other subsurface remediation technologies and have applicability to a wide range of contaminants. PRBs can be operated in an active mode where movement of groundwater is controlled by pumps or in a passive mode where the existing hydraulic gradient moves the groundwater through the reactive material. Currently two basic types of configurations are available, continuous PRB and funnel-and-gate PRB (63). Various materials have been tested as media in PRBs, e.g., Zero-Valent Iron (ZVI) (17, 25, 27, and 45), Fe (II) (3), surfactant treated zeolites (33), mixture of compost, wood chips, gravel, limestone (6). Recently, Fruchter et al. (2000) has reported creation of an in-situ permeable reactive zone by subsurface redox manipulation with injection of chemicals. Since PRB technology is still in its development stage, little research has been done to investigate its potential problem areas and to measure its long-term performance (17, 25, 35, and 45).

Potential problems associated with PRBs include, but are not limited to, corrosion of iron with subsequent chemical precipitation and biofouling. Both of these problems have the potential to substantially impact the hydraulic capture zone, the residence time in the reactive zone, and cause buildup of hydraulic pressures on the upstream side of the reactive zone. Chemical precipitation can result when redox sensitive ions change state due to changes in alkalinity or other water chemistry parameters, viz. increase in ferrous and sulfide concentrations (34). Since most research has focused on chemical precipitation, knowledge about biofouling of PRBs is limited.

Biofouling can occur due to enhanced microbial growth within the reactive zone (6, 25). It is initiated by the adsorption of microorganisms to the subsurface media. Bacterial adsorption can be considered to take place in four phases (62). First, the bacterium transfers to the solid surface, via diffusion, convection, or active transfer by chemotaxis. Second, initial adhesion consisting of a reversible followed by an irreversible phase occurs. Third, the bacterium firmly attaches through the synthesis of specialized structures. Fourth, surface colonization begins. The initial adhesion step is typically considered a primarily physicochemical phenomenon that can be described by colloid stability theory, such as the classical Derjaguin, Landau, Verwey, & Overbeek (DLVO) (40) theory. The traditional DLVO forces consist of an electrodynamic or Lifshitz-van der Waals component (LW) and an electrostatic component (EL). A number of

researches have described bacterial adhesion to different surfaces using DLVO theory (8, 66, 69), where bacterial cells were treated as inert colloids. However, in a number of cases DLVO theory alone has been found inadequate to describe behavior of colloids in suspension (72, 82). Recently, van Oss and colleagues have reported a missing component in the DLVO force balance that accounts for aqueous interactions, the Lewis acid-base interaction (AB), and thus extended the DLVO theory (XDLVO) (72).

Recent literature describes bacterial adhesion to particles in aqueous media using XDLVO theory with good correlation to experimental observations (24, 50, 57, 70). However, the primary focus of the studies was the behavior of pure strains of bacteria in relation to their attachment to surfaces. In an actual environmental setting at a contaminated site, the subsurface biogeochemistry should allow for metabolically similar groups of bacteria to dominate the ecological community. Therefore, there is a need to examine the predominant bacterial groups to understand species interaction with each other as well as species interaction with the physical surrounding. Based on a review of current literature by the researchers, this study is the first attempt to predict biofouling potential of a subsurface reactive treatment zone considering the overall surface thermodynamic characteristics of a group of microorganisms.

C. SCOPE

The scope of this study was to develop and implement a tool to predict microbial adhesion and ultimate biofouling of PRBs using microbial surface thermodynamic characteristics, which would help assess the long-term performance of the PRBs. Dominant microbial groups were enumerated, identified, and cultured from upstream, reactive iron core, and downstream soil samples from Dover Air Force Base (DAFB), Delaware. Electrodynamic, polar and electrostatic interaction energies between the groups of microorganisms and the ZVI were quantified through contact angle and zeta potential (ζ-potential) measurements. XDLVO theory was applied to determine adhesion characteristics of the microorganisms to ZVI and to predict potential for biofouling of PRBs.

D. METHODOLOGY

The major microbial groups were identified using selective (or elective) culture techniques to isolate different types of bacteria from the soil cores. All samples were analyzed for the possible presence of five different groups of microorganisms: $NO3^-$-reducers, SO_4^{-2}-reducers (SRB), Fe (III)-reducers (IRB), anaerobic heterotrophs (ANA), and aerobic (facultative) heterotrophs (AER). The concentrations of viable cells were estimated by the most probable number (MPN) method (11, 47). All anaerobic work was done inside an anaerobic chamber with 90:10 (volume basis) N_2: H2 atmosphere.

Detection of NO_3^--reducers was done through amendment of the samples with 0.1% KNO_3 in serum bottles. Loss of NO_3^- was traced by analyzing samples from the serum vial using a Dionex® 2010i-ion chromatograph. SRB and IRB were enumerated in Hungate-type culture tubes using Postage's Medium F (4) and medium described by Ghiorse (23) respectively, following 5-tube most probable number (MPN) technique (11, 47). Headspaces of the tubes for SO_4^{-2}-reduction were kept pressurized at 5 psi with 80:20 (volume basis) H_2: CO2 in a Hungate

gas station. All tubes were incubated for 30 days at 35°C with periodic manual agitation. Positive tubes for SO_4^{-2}-reduction were indicated by black precipitate and those for Fe (III)-reduction were indicated by a change in color of the Fe slurry to dark brown from reddish brown. ANA were enumerated using Bacto® Anaerobic Agar following plate count method. The agar plates were incubated in BBL Gas Pak® System anaerobic jars at 35°C for 4 days. AER were enumerated using Bacto® R2A agar following plate count method. The agar plates were incubated at 28°C for 7 days (2).

The surface tension parameters and surface potentials for the microorganisms (biotic surfaces) and the zero valent iron (abiotic surface) were quantified using contact angle and zeta-potential (ζ) measurements and with the application of theory described in the materials and methods section. The advancing contact angles and ζ-potentials of SRB, ANA, and AER cultured from the ZVI were determined at mid-logarithmic growth, stationary, and decay-states. These states, for all bacteria, were determined based on optical density readings at 660 nm (OD_{660}) using a HACH DR/2000 spectrophotometer. SRB consortium was cultured using slightly modified Tanner's medium (59); ANA were cultured using Bacto® Anaerobe Broth MIC (DIFCO Laboratories, MI); AER were cultured in a hydrocarbon minimal medium. Advancing contact angles for the cells were determined using procedures described by Grasso, et al. (24) using a Tantec Contact Angle Meter (Tantec, IL). Four different liquids were used of which diiodomethane was apolar and water, formamide, and glycerol were polar. For each liquid, an average of 10 readings was recorded. Zeta potential of the cells were measured directly using the Lazer Zee Meter®, Model 501 (Pen Kem Inc., NY). The washed cells were first suspended in DI water to a concentration of approximately 10^6 cells/ml. Numbers of cells in the suspension were counted using a Hemacytometer (Hausser Scientific Company, PA) under 1000x magnification.

ZVI surface free energy determination was done through contact angle measurements by column wicking method. Washburn equation (79) was used for the calculation of contact angles. Three different probe liquids were used for contact angle measurements, diiodomethane, water, and formamide. Hexane was used as a spreading liquid due to its very low surface tension (78). ζ-Potential measurements were done using Lazer Zee Meter®, Model 501 (Pen Kem Inc., NY). An average of 10 readings under an applied potential of 100 V was recorded.

For partitioning experiments, SRB cells were harvested at different physiological states following same procedure as stated earlier. Partitioning experiments were done in 40-ml vials with Teflon-lined screw caps. Twenty ml of the cell suspension and 20-mg sieved (106 μm) ZVI were combined in each vial. All vials were shaken in a rotary shaker at 80 rpm and at room temperature for 30 minutes. The contents of the vials were then filtered through MSI® 25-mm nylon filters of 5 μm size and the OD_{660} values were measured. OD_{660} reductions in the samples were calculated as a percent of the initial OD_{660} and averages of five experiments were recorded.

E. RESULTS AND DISCUSSION

SRB were the predominant group of microorganisms in ZVI and their numbers were approximately 2 to 4 orders of magnitude higher than in upstream and downstream locations. However, in ZVI, ANA count was approximately two orders of magnitude lower. AER count

was lower than SRB and ANA at upstream and reactive core locations. AER were not detected at downstream location. No viable IRB or NO_3^--reducing microorganisms were detected in any of the samples. Subsurface chemistry showed an oxidation-reduction potential (ORP) around -300 mV and dissolved oxygen (DO) concentration around 0.30 mg/L in ground water samples collected from the reactive core at DAFB.

Our finding that SRB are the predominant organisms in the ZVI is in accordance with the subsurface redox chemistry at the site (32, 80). SRB are an important group of morphologically very closely related anaerobic microorganisms which have been shown capable of dehalogenation of different chlorinated solvents including TCE, PCE, DCE and also degradation of petroleum BTEX compounds by various researchers (7, 9, 10). Gu et al. recently reported microbially mediated iron-sulfide precipitate in ZVI columns (25). Higher counts of SRB in the reactive zone compared to upstream and downstream locations, therefore, indicate that the actual degradation of the contaminants is possibly coupled to microbial sulfate reduction in the reactive zone. In that case, iron-sulfide precipitate could cause clogging problems of the permeable barrier at DAFB site. Since ANA population at upstream location is very high, ANA have potential to be transported to the reactive core. However, once they reach the reactive core they have to compete with the SRB, which are already the dominant populations within the reactive zone. AER count in the ZVI is around two orders of magnitude lower than the SRB and one order of magnitude lower than the ANA. This result is expected because of low DO values in the reactive zone.

Zeta potentials measured for the different groups of bacteria at different physiological states varied between –11.5 (ANA at logarithmic state) to –21.3 (ANA at decay-states). However, all measured values stayed within the range of <25 mV at which the equations for determining the EL components of ΔG_{1W1} and ΔG_{1W2} are valid (72). These results conform to the findings reported by Smets et al. (57). The LW component of the surface tension (γ^{LW}) did not show large variation (standard deviation 2.37) among different consortia at different physiological states. This result conformed to the findings reported by other researchers (24, 57). Lowest γ^{LW} (40.61 mJ/m^2) was observed for SRB at stationary state and the highest γ^{LW} (46.51 mJ/m^2) was observed for the same at decay-state. At all physiological states, the electron acceptor surface tension parameter (γ^+) of ANA were around one mJ/m^2 and the electron donor parameter (γ^-) were >28.5 mJ/m^2. Thus, ANA exhibited a monopolar hydrophilic surface (72, 74) at all states. However, for SRB and AER, γ^+ values were much greater than one mJ/m^2 and γ^- values were within 25.17 to 33.56 mJ/m^2 at all physiological states. Thus, SRB and AER did not show a dominant monopolar surface characteristic at any state. ZVI had a relatively low γ^{LW} value. The γ^+ value of 2.47 mJ/m^2 and γ^- value of 16.87 mJ/m^2 showed that the ZVI surface was not monopolar (72, 74). The measured ζ–potential of ZVI (-12.1 mV) was within moderate range of <25-mV (72).

Only SRB at logarithmic state and AER at stationary state manifested hydrophobic cell surface characteristics. As the SRB cells went from logarithmic to stationary state, their cell surface characteristic changed from hydrophobic to hydrophilic. The cells became more hydrophilic from stationary to decay-states. ANA cells also showed a somewhat similar trend, where the cells became more hydrophilic as they went from logarithmic to stationary and from stationary to decay-state. However, AER cells became hydrophilic to hydrophobic as they went

from logarithmic to stationary state. The cells became hydrophilic again as they entered decay-state. Hydrophilicity of AER cells in decay-state was more than in logarithmic state.

The ExDLVO plots suggests that for SRB at small separation distances (approximately <10 Å), the AB forces dominated and the cells showed negative ΔG_{1W2} values at all physiological states. In logarithmic state, highest negative free energy was observed. Magnitude of ΔG_{1W2}^{TOT} in stationary state was the lowest but similar to the magnitude of ΔG_{1W2}^{TOT} at decay-state. This indicated highest adhesion potential of SRB cells to ZVI surface at logarithmic state and lowest potential for adhesion at stationary state. The ΔG_{1W2}^{TOT}-values for ANA remained positive at all separation distances and at all physiological states. At small separation distances, AB forces dominated and the magnitude of ΔG_{1W2}^{TOT} increased as the cells went from logarithmic to stationary and from stationary to decay-state. Thus, ANA showed decreasing adhesion potential to ZVI surface as the cells went from logarithmic to stationary and from stationary to decay-states. For AER at short distances, highest negative free energy was observed for cells in stationary state, where AB forces dominated. AER showed highest adhesion potential to ZVI surface at stationary state and lowest at decay-state. Because decays of LW and EL forces were very rapid, at larger separation distances (approximately >25 Å) the EL forces dominated and decay of G_{1W2}^{TOT} was very gradual for all consortia at all physiological states.

An interesting behavior of SRB, the dominant group of microorganisms in the reactive core, is worth noticing. SRB cells showed highest hydrophobicity (indicated by ΔG_{1W1}^{TOT} calculations) and correspondingly the highest adhesion potential (indicated by ΔG_{1W2}^{TOT} calculations) at logarithmic state. However, although the cells at decay-state were more hydrophilic than cells at stationary state, at short distances decay-state cells showed more adhesion potential to ZVI compared to cells in stationary state. This result is contrary to the reports of a number of authors, who described surface hydrophobicity/hydrophilicity as the only measure for adhesion of cell to surfaces (24, 58, 65). The theoretical observations were validated through partitioning experiments.

Partitioning of SRB at different physiological states between suspended and attached to ZVI phases was measured as a percent reduction of OD_{660}. Highest partitioning (26.5%) was observed at logarithmic state. At stationary state, partitioning of bacteria was lowest (14.1%) and was almost half of that at logarithmic state. Decay-state partitioning (17.0%) was closer to but higher than that at stationary state. The results also showed greater partitioning of cells at decay-state compared to the cells at stationary state. Consequently, the results from the partitioning experiments confirmed the predicted adhesion of SRB to ZVI by the XDLVO calculations.

F. CONCLUSIONS

The few PRB long-term performance studies mostly focused on the chemical aspect of the reactive core. The observed flow reductions and performance deterioration typically was postulated as a result of chemical precipitation. Although biofouling was observed in Newbury Park, CA (53) and Portsmouth, OH (35), a model for predicting the potential for such biofouling in PRBs was not present. Our study shows that the dominant SRB population at DAFB site

permeable reactive core has the potential for biofouling, which can be predicted by a bacterial surface-thermodynamics approach. This report thus presents an optimal method for the prediction of biofouling potential and assessment of long-term microbiological performance of PRBs.

TABLE OF CONTENTS

LIST OF FIGURES

LIST OF TABLES

SECTION I
INTRODUCTION

A. OBJECTIVE

The goal of this research is the development and implementation of microbial surface thermodynamic technology that can be used to predict microbial adhesion characteristics and ultimate biofouling. This goal is achieved via identification of dominant microbial groups up-gradient, within and down-gradient of a reactive barrier, enumeration of identified microbial groups, and quantification of electrodynamic and electrostatic surface potentials of dominant microbial groups.

B. BACKGROUND

1. General

Sorptive reactive treatment zones can be used *in-situ* (e.g., with columns or walls of porous media intercepting existing groundwater flow paths) or *ex-situ* (e.g., in above ground porous media bioreactor, through which contaminated groundwater is pumped). The *in-situ* technology can be passive or active. When operated in the passive mode, the existing hydraulic gradient moves groundwater into the sorptive reactive porous media. When utilized in the active mode, pumps move groundwater through the media; this can be accomplished using *in-situ* or *ex-situ* and can be combined with other technology (e.g., surfactant-enhanced elution). Mixtures of sorptive material, iron and/or sulfate containing minerals and granular inert materials (e.g., quartz sand) are used to create a porous media with the desired sorptive, biodegradation, and hydraulic conductivity properties. As contaminants move into the treatment zone, contaminant migration is slowed by the sorptive material, increasing residence time in the media. Biosynthesis and bioenergetic pathways of bacteria are facilitated by oxidation-reduction reactions involving contaminants and Fe^{3+} or SO_4^{2-}. Thus, these redox reactions in anaerobic environments result in contaminant degradation.

Potential problems associated with these systems include, but are not limited to, chemical precipitation and biofouling, both of which could substantially impact the hydraulic capture zone and residence time. Chemical precipitation can result when redox sensitive ions change state due to changes in alkalinity (or other water chemistry parameters such as increase ferrous and sulfide concentrations). Enhanced anaerobic microbial growth occurring in the reactive barrier would also impact the hydraulic flow patterns or result in reactive wall plugging. Biofouling can be initiated as a result of microbial adhesion or biomass sloughing, both are related to mechanisms that govern microbial transport.

2. Microbial Adhesion

The movement of bacteria through porous geological formations is a critical factor in the fate and remediation of many polluted surface and subsurface formations (22, 31, 61, and 83). Prediction of contaminant fate therefore requires accurate incorporation of factors governing bacterial transport phenomena. Bacterial transport is also important when the bacteria

themselves are of concern because the microorganisms are expected to cause biofouling of many abiotic treatment processes. This background section summarizes and discusses previous work and concepts in bacterial adhesion as they relate to the proposal objectives.

Adsorption can be considered to take place in four phases (30, 41, 62, 69). First, the bacterium transfers to the solid surface, via diffusion, advection, or active transfer by chemotaxis. Second, initial adhesion occurs consisting of a reversible followed by an irreversible phase. Third, the bacterium firmly attaches through the synthesis of specialized structures. Fourth, surface colonization begins. Initial adhesion is typically considered a primarily physicochemical phenomenon. According to some, initial bacterial adhesion is reversible and takes place in the secondary total interfacial energy minimum (8, 69). The illustrated importance of electrostatic parameters (e.g., electrokinetic potential of the particle or surface and medium ionic strength) has strongly corroborated this notion (21, 40, 43, 44). However, the distance between the secondary adsorption minimum and the solid surface has been reported to be too large to allow immediate surface interaction (69). Long range hydrophobic forces must therefore play a major role in adhesion (18, 42, 58, 64).

The essential physicochemical parameters thought to govern adsorption behavior have been quantified via several different experimental assays. Electrostatic character has mainly been measured using zeta potentials (13, 21, 39, 44, 52, 64), and ion exchange chromatography (21, 32). Hydrophobicity has been measured using contact angle measurements (8, 13, 18, 39, 44, 49, 52, 65), hydrophobic interaction chromatography (21, 32), and several different partitioning assays (5, 13, 20, 31, 43, 65).

Four studies used complicated retardation approaches when modeling microbial adhesion. It appears to date; few have incorporated colloid stability theory. For example the classical Derjaguin, Landau, Verwey, & Overbeek (DLVO) theory--which considers van der Waals and electrostatic interactions--and none have incorporated extended DLVO theory--which also considers long range hydrophobic (Lewis acid/base) forces. Lindqvist and Bengtsson (37) used a two-site model, which involved an instantaneous, linear equilibrium site and a reversible, linear kinetic site. Lindqvist et al. (38) assumed that sorption rate was a function of the water-phase bacterial concentration and the number of available sites on the soil, while desorption was proportional to soil-sorbed bacterial concentration. Taylor and Jaffé (60) depicted the attached biomass as a thickening biofilm exposed to shearing, and the rate of deposition of bacteria was linear with respect to solution-phase bacterial concentration. Finally, Zysset et al. (84) also depicted attached mass as a biofilm, modeled sorption by a first order rate expression, but related desorption to the growth rate of the attached biomass. None of the authors above, however, took a detailed mechanistic approach to investigate the causes of initial attachment.

3. Surface Thermodynamics

Classical DLVO theory has often been used to describe interfacial interactions in modeling of particle transport. Traditional DLVO forces are comprised of an electrodynamic or van der Waals component and an electrostatic component. A recent study reported that the experimentally determined colloidal attachment efficiency of an abiotic Brownian particle in porous media was several orders of magnitude larger than predicted by classical DLVO theory.

This discrepancy was attributed to potentially one or more of the following: interfacial electrodynamics of interaction, coupling of electrodynamics and hydrodynamics, and surface roughness. In a subsequent theoretical paper, the previous model was modified by accounting for surface charge heterogeneity. Several other studies have also reported that classical DLVO theory was often inadequate in describing colloidal stability as well as bacterial adhesion.

It has been surmised that physical interactions, other than electrodynamic and electrostatic, play a major role in colloid stability in aqueous media. Van Oss and Israelachvili, using different techniques, have both identified an additional (hydrophobic) force component that has hitherto been neglected in the DLVO force balance. Van Oss and colleagues have extended DLVO (ExDLVO) theory by accounting for Lewis acid-base interactions. Lewis acid/base interactions include chemical phenomena described by the Arrhenius, solvent system, Lux-Flood, and proton acid-base definitions. Traditional coordination chemistry; non-classical complexes, such as, solvation and solvolysis; nucleophilic and electrophilic reactions; charge transfer complexes; weak intermolecular forces and H-bonding, and hydrophobic partitioning. Electron donor, donor/acceptor interactions are asymmetric in nature and can be either repulsive or attractive. The inclusion of acid-base forces is essential for describing polar media interfacial interactions.

When van Loosdrecht et al. (69) attempted to correlate bacterial adhesion to negatively charged polystyrene (in a non-flow apparatus) with bacterial electrophoretic mobility (traditional DLVO approach), they reported that no clear correlation was observed. Rather, bacterial surface hydrophobicity was the dominant characteristic in determining adhesion. This clearly supports the need for an ExDLVO approach to modeling interactions.

However, many bacterial strains have the ability to produce exopolymers, which can be retained in their glycocalyx or exuded into the environment and adhere onto solid surfaces themselves. Consequently, bacteria may encounter surfaces that are not characterized by the original matrix chemistry, but rather have been preconditioned with exopolymers. The resulting bacterium/particle interaction will then depend on the surface thermodynamics of the exopolymer-coated particle.

The surface thermodynamic properties deriving from the dynamic interaction between the bacterium (1) and a surface (2) in water (w) must be measured in order to understand and predict their net interaction. Lifshitz-van der Waals (LW) work of adhesion (W_{1W2}^{LW}), Lewis acid-base (AB) work of adhesion (W_{1W2}^{AB}), and the work of electrostatic interaction (W_{1W2}^{EL}).

The LW work of adhesion of bacteria is given by:

$$W_{1W2}^{LW} = \gamma_{1W}^{LW} + \gamma_{2W}^{LW} - \gamma_{12}^{LW} \qquad (1)$$

Where γ_i^{LW} is the Lifshitz-van der Waals, or apolar, component of the surface tension of material (i), and where

$$\gamma_{ij}^{LW} = \left(\sqrt{\gamma_i^{LW}} - \sqrt{\gamma_j^{LW}}\right)^2 \quad (2)$$

When 2 is a condensed-phase material (e.g., sand, silica, or clay, etc.), W_{1W2}^{LW} is always positive, i.e., attractive. W_{1W2}^{LW} is typically small compared to W_{1W2}^{AB}. The AB work of adhesion is,

$$W_{1W2}^{AB} = \gamma_{1W}^{AB} + \gamma_{2W}^{AB} - \gamma_{12}^{AB} \quad (3)$$

Where $\gamma_i^{AB} = 2\sqrt{\gamma_i^+ \gamma_i^-}$ and γ_i^+ is the electron-acceptor and γ_i^- the electron-donor parameter of the polar γ_i^{AB} surface tension component of material (i) and

$$\gamma_{ij}^{AB} = 2\left(\sqrt{\gamma_i^+ \gamma_i^-} + \sqrt{\gamma_j^+ \gamma_j^-} - \sqrt{\gamma_i^- \gamma_j^+} - \sqrt{\gamma_i^+ \gamma_j^-}\right) \quad (4)$$

The γ_i^{LW}, γ_i^+, and γ_i^- components are measured together, by means of contact angle (θ) determinations, as outlined in the protocol section.

In a number of cases, when the average electrokinetic or ζ-potentials of bacteria (1) and particles (2) exceeds 10 to 12 mV, ζ-potentials of bacteria and particles need to be determined, usually by means of microelectrophoresis. The work of electrostatic interaction, W_{1W2}^{EL}, then can be determined in the manner described in the experimental section.

The interfacial (IF) work of interaction is

$$W_{1W2}^{IF} = W_{1W2}^{LW} + W_{1W2}^{AB} \quad (5)$$

While the total work of interaction then is

$$W_{1W2}^{TOT} = W_{1W2}^{IF} + W_{1W2}^{EL} \quad (6)$$

One may also include the Brownian motion work (W^{BR}), but the value of this is always on the order of 1 kT. Since W^{BR} energy is, therefore, typically one to two orders of magnitude smaller than that associated with AB or LW energies are neglected.

All three forces (LW, AB, and EL) can act at non-negligible distances in aqueous media. Because each type of force decays with distance between the bacterium and particle with different spatial dependencies, energy versus distance plots (taking LW, AB, and EL forces into account) must be defined to predict adhesion. For spherical geometries, W^{LW} decays occur proportionally to the inter-surface distance, ℓ, whereas W^{AB} and W^{EL} decay exponentially. W^{AB} as exp ($-\ell/\lambda$) and W^{EL} as exp ($-\ell\ \kappa$), where λ is the decay length of water and $1/\kappa$ the electrokinetic decay length, or Debye length, which is inversely proportional to the square root of the ionic strength of the medium. Thus, bacteria or particles with speculations, sharp edges, or

other protrusions with a small effective radius can more easily overcome a net macroscopic repulsion than completely smooth particles. In this manner, they can engage in adhesion via microscopic sites located at the distal ends of such protrusions.

Three generalizations may be made with respect to the surface thermodynamics of macroscopic bacterial adhesion. First, W^{LW} is always positive (attractive) in aqueous media at non-air interfaces, and relatively little can be done to influence its value significantly.

Additionally, W^{LW} is small usually compared to other parameters. Second, W^{EL}, as far as macroscopic interactions are concerned, is usually negative (repulsive). Its absolute value is decreased by an increase in the ionic strength, changes in (usually decreasing) pH, or the presence of multivalent counterions. Finally, W^{AB} can be negative (repulsive) in cases of interactions between hydrophilic cells and particles, or positive (attractive) when at least one of the interacting materials is hydrophobic. Very hydrophilic surfaces have a low to zero γ^+ and a high γ^- value ($\gamma^- > 28$ mJ/m^2). Hydrophobic surfaces (also with a low to zero γ^+) have a $\gamma^- < 28$ mJ/m^2. When the ζ-potential of bacteria, particles, or biopolymers is lowered, their Lewis acid-base properties are impacted as well. With decrease in the ζ-potential, the AB parameter, γ^-, decreases concomitantly, via a newly identified one-way EL-AB linkage. Thus, bacterial adhesion to mineral particles can usually be enhanced by the admixture of, $CaCl_2$, for example, in low concentration (e.g., 10^{-2} M).

C. SCOPE

The scope of this study was to develop and implement a tool to predict microbial adhesion and ultimate biofouling of PRBs using microbial surface thermodynamic characteristics, which would help assess the long-term performance of the PRBs. Dominant microbial groups were enumerated, identified, and cultured from upstream, reactive iron core, and downstream soil samples from Dover Air Force Base (DAFB), Delaware. Electrodynamics, polar and electrostatic interaction energies between groups of microorganisms and ZVI were quantified through contact angle and zeta potential (ζ-potential) measurements. XDLVO theory was applied to determine adhesion characteristics of the microorganisms to ZVI and to predict potential for biofouling of PRBs.

D. APPROACH

Identification of major microbial groups will coincide with their enumeration in the soil cores. Specific microbial groups expected at the site include (but not limited to) sulfate-reducing bacteria, iron-reducing bacteria, anaerobic fermenters, aerobic/facultative heterotrophs, and methanogens. Other trophic groups, such as autotrophic denitrifiers, will also be examined; however, the aforementioned groups are the predicted dominant and representative bacterial groups present at the site. The following section describes a brief narrative of the microbial identification, enumeration, and cell hydrophobicity methodology proposed.

1. Microbial Identification

The major microbial groups were identified using selective (or elective) culture techniques to isolate different types of bacteria from soil cores. This consists of about 18 biochemical assays and 25 assimilation tests in addition to standard microbial microscopic examinations. These tests are designed for use on Gram-negative: *Enterobacteriaceae*, Gram-negative: non-*Enterobacteriaceae*, Gram-positive: staphylococci, Gram-positive: streptococci, and anaerobic microorganisms.

The selective culture technique was used to identify sulfate-reducing bacterial (SRB), iron-reducing bacteria (IRB), and nitrate-reducing bacteria, anaerobic heterotrophs (ANA) and aerobic heterotrophs (AER). For SRB, Postgate's medium F (47) will be used. Medium will be prepared using the Hungate type anaerobic culture tubes under strictly anoxic conditions. Tubes will be incubated at 35°C for 30 days. For IRB, medium described by Ghiorse (23) will be used. Tubes will be incubated at 35°C for 30 days. ANA will be enumerated using Bacto® Anaerobic Agar (DIFCO Laboratories, MI) following plate count method. The agar plates were incubated in BBL Gas Pak® System anaerobic jars at 35°C for 4 days. AER were enumerated using Bacto® R2A agar (DIFCO Laboratories, MI) following plate count method. The agar plates were incubated at 28°C for 7 days.

2. Microbial Enumeration

The concentration of viable cells can be estimated by the most probable number (MPN) method (11, 47). This involves the mathematical inference of the viable count from the fraction of cultures that fail to show growth in a series of broth medium. This method consists of making several replicate dilutions in a growth medium and recording the fraction of tubes showing bacterial growth. The tubes exhibiting no growth presumably failed to receive even a single microorganism that was capable of growth. Since the distribution of such particles must follow a Poisson distribution, the mean number at this dilution can be calculated from the formula:

$$P_0 = e^{-m} \tag{7}$$

where m is the mean number and P_0 is the ratio of the number of tubes with no growth to the total number of tubes. The mean number is then simply multiplied by the dilution factor and by the volume inoculated into the growth tube to yield the viable count of the original culture.

The MPN method has been selected (although labor intensive) due to the uncertainty of agar viability. Second, due to the heterogeneity of sample soil cores, the kinetics of growth tends to be highly variable. Since no prior knowledge of specific microbial group concentration, tube dilution (10 fold series) will be used. For this approach, we will discard the data from dilution where the percentage of sterile tubes lies outside of 8 to 36%, or outside of the range of 5 to 50% if a large range of error is required. The error from the dilution with the range can be read or interpolated from standard coefficient of error curves statistically generated for the MPN method.

3. Microbial Surface Thermodynamics

Surface thermodynamic properties were determined using a variety of techniques. The electrostatic component of particle surface forces was determined directly by using a Lazer Zee Meter®, Model 501 (Pen Kem Incorporated, NY). At least 10 readings were taken to have consistency in measured values and the measurements will be conducted under an applied potential of 100 V.

Surface tension measurements were used to quantify Lewis acid/base and Liftshitz-van der Waals forces. Upon filtering suspension on a silver membrane, a smooth flat layer will form, on which contact angles (θ) can be measured, yielding γ_i^{LW}, γ_i^+, and γ_i^- as outlined below.

Surface tension components from the contact angles (θ) are measured with liquid (L) on surfaces (S), using the following version of Young's equation (73):

$$(1+\cos\theta)\gamma_L = 2\left(\sqrt{\gamma_S^{LW}\,\gamma_L^{LW}} + \sqrt{\gamma_S^+\,\gamma_L^-} + \sqrt{\gamma_S^-\,\gamma_L^+}\right) \tag{8}$$

Where γ_L is the total surface tension of the liquid, γ_i^{LW} the Lifshitz-van der Waals (LW) or apolar component of condensed material (i), γ_i^+ the electron acceptor and γ_i^- the electron donor parameter of the Lewis acid-base (AB), or polar component of the surface tension. Here,

$$\gamma_i^{AB} = 2\sqrt{\gamma_i^+\gamma_i^-} \tag{9}$$

and

$$\gamma_i = \gamma_i^{LW} + \gamma_i^{AB} \tag{10}$$

which can be determined using liquids with known surface thermodynamic properties. As there are three unknowns in the above Young's equation for the surface properties of a given solid (S), contact angle (θ) determinations must be done with at least three high energy liquids, of which at least two must be polar. It is proposed herein to use glycerol and/or formamide as the polar liquids and diiodomethane as the apolar liquid. A Tantec Contact Angle Meter (Tantec, IL) was used to acquire a minimum of 10 advancing contact angle measurements per sample.

SECTION II
MATERIALS AND METHODS

A. THEORITICAL CONSIDERATIONS

The theories of colloidal interactions in aqueous media have been described in detail by different authors (28, 29, and 72); a detailed discussion is not presented herein. Only the theories and model development relevant to microbial adhesion to surfaces are presented. The primary non-covalent forces that play a major role in particle-particle interaction in a liquid media are LW forces, AB forces, EL forces, and Brownian (BR) movement forces (70, 72). However, the BR forces are usually a few orders of magnitude smaller than the other three forces. It can thus be safely neglected while calculating force balance for describing bacterial adhesion to surfaces or bacterial stability in water (70).

The free energy of interfacial interaction between two similar particles (1) immersed in water (W), i.e. ΔG_{1W1} expressed in kT units is a suitable measure for the prediction of stability of particles in aqueous suspensions (72). Here, k is the Boltzmann's constant (1.38×10^{-23} J/degree Kelvin) and T is the absolute temperature in degrees Kelvin. A value of $\Delta G_{1W1} < 0$ would indicate hydrophobicity and less stability of particles; whereas, a value >0 would indicate hydrophilicity and more stability of the particles (72). The total interaction energy ΔG_{1W1}^{TOT} is a summation of its LW, AB and EL components. For all 1W1-type interactions, the bacterial cells can be approximated as small cylinders.

The LW component of ΔG_{1W1}^{TOT} between two cross cylinders at 90° separated at a distance l_0, is given by:

$$\Delta G_{1W1}^{LW} = -4\pi l_0 R \left(\sqrt{\gamma_1^{LW}} - \sqrt{\gamma_3^{LW}}\right)^2 \tag{11}$$

where γ_i^{LW} stands for the apolar component of the surface tension of substance i. The distance, l_0 is the minimum equilibrium distance between the two particles of material one immersed in water, which is approximately 1.57 Å (76).

The polar or AB component of ΔG_{1W1}^{TOT} between two cross cylinders at 90° separated at a distance l_0, is given by:

$$\Delta G_{1W1}^{AB} = 2\pi R \lambda \Delta G_{1W1,l_0}^{AB} \tag{12}$$

where λ is the characteristic length or decay length of the liquid, which for water can be fairly approximated as 0.6 nm (71). $\Delta G_{1W2,l_0}^{AB}$ is the Lewis acid-base energy of interaction between two semi-infinite flat plates immersed in a liquid and at a distance l_0, expressed as:

$$\Delta G_{1W1,l_0}^{AB} = -4 \left(\sqrt{\gamma_1^+} - \sqrt{\gamma_3^+}\right)\left(\sqrt{\gamma_1^-} - \sqrt{\gamma_3^-}\right) \tag{13}$$

where γ_i^+ and γ_i^- are the electron-acceptor and electron-donor parameters of the surface tension of substance i.

The surface tension components γ_i^{LW}, γ_i^+ and γ_i^- for solids can be calculated by contact angle measurements on the solid's surfaces and with the help of equation 8. In that equation the surface tension of the liquid, γ_L, is expressed as:

$$\gamma_L = \gamma_L^{LW} + 2\sqrt{\gamma_L^+ \gamma_L^-} \tag{14}$$

In equation 8 there are only three unknown variables, γ_S^{LW}, γ_S^+, and γ_S^-, which can be determined by measuring contact angles on the solid surfaces with at least three different liquids whose surface tension components are known. At least one of the liquids needs to be apolar. For the polar liquid, the γ_L^+ and γ_L^- components equal zero. This facilitates the determination of γ_s^{LW} directly from equation 4 without complicated calculations.

Assuming constant surface potential, the electrostatic or EL component of ΔG_{1W1}^{TOT} between two cross cylinders at 90° separated at a distance l_0 (for ψ<50 mV), is given by:

$$\Delta G_{131}^{EL} = 2\pi\varepsilon\varepsilon_0 R\psi_1^2 [\ln\{(1+\exp(-\kappa l_0))/(1-\exp(-\kappa l_0))\} + \ln\{1-\exp(-2\kappa l_0)\}] \tag{15}$$

where ε is the relative dielectric constant of the liquid (80.18 for water at 20°C), ε_0 is the permittivity of free space (8.85×10^{-12} C^2/m-J), R is the radius of the cylinders, ψ_i is the potential of particle of material i at the particle-liquid interface. Although ψ_i is not directly measurable, it can be calculated from zeta potential (ζ) as follows:

$$\psi = \zeta\,(1+z/a)\exp(\kappa z) \tag{16}$$

where z is the distance from the particle surface to the slipping plane (approximately 3-5Å) (72) and a is the radius of the particles. The zeta potential can be measured by different methods; a detailed overview is given by Righetti, et al. (48).

The Debye length, $1/\kappa$ in equations 6 and 7 is an estimate of the effective thickness of the electric double layer, which is 1,000 nm for pure water. However, its value depends on the ionic strength of the liquid as:

$$1/\kappa = [(\varepsilon kT)/(4\pi e^2 \sum v_i^2 n_i)]^{1/2} \tag{17}$$

where e is the charge of an electron (4.8×10^{-10} e.s.u.), v_i is the valency of each ionic species, and n_i is the number of ions of each species in bulk liquid per cm^3.

The free energy of interfacial interaction between bacterial cells and attachment surface immersed in water, i.e. ΔG_{1W2}, provides a measure for attachment potential of the microorganisms to the surfaces (72). In our case, the attachment matrix is the ZVI chips that are of sizes at least an order of magnitude larger than the bacteria. Thus, the type of interaction between the bacterial cells and the ZVI can be considered as sphere-plate interaction. The LW, AB, and EL components of energy of interaction between a sphere of radius R (material 1) and a

semi infinite flat plate (material 2) immersed in water at a separation distance l are given by the following equations:

$$\Delta G_{1W2}^{LW} = -4\pi l_0^2 R \left(\sqrt{\gamma_1}^{LW} - \sqrt{\gamma_3}^{LW}\right)\left(\sqrt{\gamma_2}^{LW} - \sqrt{\gamma_3}^{LW}\right) / l \quad (18)$$

$$\Delta G_{1W2}^{AB} = 2\pi R\lambda \Delta G_{1W2,l_0}^{AB} \exp[(l_0 - l)/\lambda] \quad (19)$$

$$\Delta G_{1W2}^{EL} = \pi\varepsilon\varepsilon_0 R \left[2\psi_1\psi_2 \ln\{(1+\exp(-\kappa l))/(1-\exp(-\kappa l))\} + (\psi_1^2 + \psi_2^2)\ln\{1-\exp(-2\kappa l)\}\right] \quad (20)$$

On an average, R was approximated as 1 μm for the cells in a consortium. $\Delta G_{1W2,l_0}^{AB}$ is the Lewis acid-base interaction energy between two semi-infinite flat plates immersed in water and at a distance of l_0, which is expressed as:

$$\Delta G_{1W2,l_0}^{AB} = 2\left[\left(\sqrt{\gamma_1}^{+} - \sqrt{\gamma_2}^{+}\right)\left(\sqrt{\gamma_1}^{-} - \sqrt{\gamma_2}^{-}\right) - \left(\sqrt{\gamma_1}^{+} - \sqrt{\gamma_3}^{+}\right)\left(\sqrt{\gamma_1}^{-} - \sqrt{\gamma_3}^{-}\right) - \left(\sqrt{\gamma_2}^{+} - \sqrt{\gamma_3}^{+}\right)\left(\sqrt{\gamma_2}^{-} - \sqrt{\gamma_3}^{-}\right)\right] \quad (21)$$

Equation 21 assumes constant surface potential and is valid when ψ<50 mV) (54).

The interaction energies expressed by equations 18, 19, and 20 are all additive (71). Thus, the total interaction energy can be expressed as:

$$\Delta G_{1W2}^{TOT} = \Delta G_{1W2}^{LW} + \Delta G_{1W2}^{AB} + \Delta G_{1W2}^{EL} \quad (22)$$

A negative value of ΔG_{132}^{TOT} will favor adhesion between particles of different materials immersed in aqueous media, whereas, a positive value will cause repulsion between the same. In addition, the magnitude of the total interaction energy will determine the strength of either attraction or repulsion.

B. SITE AND SAMPLE SOIL DESCRIPTION

The DAFB site is located in Kent County, Delaware. Since 1941, the site has been used for different military purposes including jet engine testing, repair, and maintenance (27). The aquifer at the site is a part of the Columbia Aquifer with a saturated thickness of 4.6-6.1 meters in the western portion of the base, to 21.3 meters in the eastern portion. The mean hydraulic conductivity at the site is 27.4 meters/day and the specific yield is 0.15 (56). Contaminants identified at the site are mainly chlorinated solvents and mono-aromatic hydrocarbons. Highest concentrations of contaminants found at DAFB site groundwater are, 1,2-dichloroethane (1,2-DCE) at 34 mg/L, trichloroethylene (TCE) at 22 mg/L, tetrachloroethylene (PCE) at 3300 mg/L, and total benzene-toluene-ethylene-xylene (BTEX) at 14200 mg/L (56). In December 1997, a funnel-and-gate type reactive permeable barrier was installed with two caisson gates to treat the contaminant plume. ZVI was used as the principal reactive material at the barrier.

The aquifer material used for the study was collected from upstream (7.92-8.08 meters depth) and downstream (5.79-5.94 meters depth) locations of the barrier. The reactive core material sample was collected at 7.62-7.77 meters depth. All samples were collected below the ground water table and stored at 4°C in an anaerobic bag for transport. After the samples arrived at the laboratory, the headspace of the sample containers was flushed with 90:10 (volume basis). N_2: H2 and stored at 4°C until analyzed.

C. ENUMERATION AND CULTURE OF MICROORGANISMS

All samples were analyzed for the possible presence of five different groups of microorganisms: NO_3^--reducers, SO_4^{-2}-reducers (SRB), Fe (III)-reducers (IRB), anaerobic heterotrophs (ANA), and aerobic (facultative) heterotrophs (AER). All anaerobic work was done inside an anaerobic chamber with 90:10 (volume basis) N_2: H2 atmosphere.

For the detection of NO_3^--reducers, 10 g (moist weight) of each sample was placed into separate serum bottles and amended with 0.1% KNO_3 (dry weight basis). The bottles were capped with thick rubber septa and crimped and were incubated at 30°C up to 14 days. NO_3^- concentration were determined at 0, 7, and 14 days. For this, 25 mL of deionized (DI) water was injected into each bottle. The bottles were then shaken for 30 minutes and the contents were filtered through Whatman® #42 filter paper. The filtrate was then passed through Osmonics 0.45-micron syringe filter and was analyzed for NO_3^- concentration using a Dionex® 2010i ion chromatograph.

SRB and IRB were enumerated in Hungate type culture tubes using Postage's Medium F (4) and medium described by Ghiorse (23) respectively, following 5-tube most probable number (MPN) technique (11, 47). Headspaces of the tubes for SO_4^{-2}-reduction were kept pressurized at 5 psi with 80:20 (volume basis) H_2: CO_2 in a Hungate gas station. All tubes were incubated for 30 days at 35°C with periodic manual agitation. Positive tubes for SO_4^{-2}-reduction was indicated by black precipitate and that for Fe (III)-reduction was indicated by a change of color of the Fe slurry from reddish brown to dark brown.

ANA were enumerated using Bacto® Anaerobic Agar following plate count method. The agar plates were incubated in BBL Gas Pak® System anaerobic jars at 35°C for four days. AER were enumerated using Bacto® R2A agar following plate count method. The agar plates were incubated at 28°C for 7 days (2).

D. SURFACE TENSION PARAMTERS AND SURFACE POTENTIALS

The surface tension parameters and surface potentials for the microorganisms (biotic surfaces) and the zero valent iron (abiotic surface) were quantified using contact angle and zeta-potential (ζ) measurements and with the application of theory described in previous sections.

1. Microorganisms

The advancing contact angles and ζ-potentials of SRB, ANA, and AER cultured from the ZVI were determined at mid-logarithmic growth, stationary, and decay states. These

states, for all bacteria, were determined based on optical density readings at 660 nm (OD_{660}) using a HACH DR/2000 spectrophotometer.

SRB consortium was cultured using slightly modified Tanner's medium (59). The amount of Fe $(NH_4)_2(SO_4)_2.6H_2O$ was adjusted to give a final concentration of 0.0017gm Fe/L of media and the amount of carbon source was halved. These modifications were done to avoid formation of black FeS precipitate during growth of the bacteria. ANA were cultured using Bacto® Anaerobe Broth MIC (DIFCO Laboratories, MI). AER were cultured in hydrocarbon minimal medium (HCMMII). The medium preparation was as follows; in g/L: KH_2PO_4 – 1.36, Na_2HPO_4 – 1.42, KNO_3 – 0.5, $(NH_4)_2SO_4$ – 2.38, $MgSO_4.7H_2O$ – 0.05, $CaCl_2$ – 0.01; in mg/L: H_3BO_3 – 2.86, $MnSO_4.H_2O$ – 1.54, $Fe(NH_4)_2SO_4.6H_2O$ – 3.53, $CuSO_4.5H_2O$ – 0.039, $ZnCl_2$ – 0.021, $CoCl_2.6H_2O$ – 0.041, $Na_2MoO_4.2H_2O$ – 0.025; pH adjusted to 7.2 with 1N NaOH; media autoclaved for 15 minutes (121°C, 15 psi); 1% sterile glucose (wt./vol.) solution added as carbon source to have a final glucose concentration of 0.05% (weight/volume) in the medium. All bacteria were cultured in Nephelo culture flasks with 200 mL of respective medium and 5% (volume/volume) inoculum. Headspaces of flasks for SRB were pressurized to 5 psi with 80:20 (volume basis) H_2:CO_2. All flasks were incubated in a rotary shaker at 35°C.

Before collecting the cultures at each physiological state, the culture flasks were allowed to sit undisturbed for 15 minutes. 40 mL of supernatant from each flask was then collected using sterile syringes and dispensed into sterile centrifuge tubes. Cells were harvested by centrifuging the tubes at 4000 rpm for 30 minutes at 4°C and washing twice with sterile PO_4-buffer ($3x10^{-4}$ M KH_2PO_4, pH adjusted to 7.0 with 1 N NaOH). Advancing contact angles for the cells were determined using procedures described by Grasso, et al. (24) using a Tantec Contact Angle Meter (Tantec, IL). Four different liquids were used of which diiodomethane was apolar and water, formamide, and glycerol were polar. For each liquid, an average of 10 readings was recorded. Zeta potential of the cells were measured directly using the Lazer Zee Meter®, Model 501 (Pen Kem Inc., NY). The washed cells were first suspended in DI water to a concentration of approximately 10^6 cells/mL. Numbers of cells in the suspension were counted using a Hemacytometer (Hausser Scientific Company, PA) under 1000x magnification. The pH of the suspension was between 6.4-6.7. The chamber of the Lazer Zee Meter® was then filled with the cell suspension and ζ-potential (average of 10 readings) under an applied potential of 100 V was recorded. A 3-minute equilibration time was allowed before taking readings. SRB and ANA were handled anaerobically throughout all procedures and deoxygenated PO_4-buffer and deoxygenated DI water were used respectively for washing these cells and making cell suspensions for ζ-potential measurements.

2. Zero Valent Iron

ZVI surface free energy determination was done through contact angle measurements by column wicking method. Washburn equation (79) was used for the calculation of contact angles (θ):

$$h^2 = \frac{R_e \gamma_L \cos\theta}{2\eta} t \qquad (23)$$

where h is the height of the liquid front at time t, R_e is the effective interstitial pore radius between the packed particles, γ_L and η are the surface tension and the viscosity of the liquid respectively. The ZVI was first passed through an USA standard testing sieve #20 to discard larger particles. It was then oven dried at 110°C overnight and cooled in a dessicator. A chemically clean glass column of 6-mm inner diameter was filled with the material up to a height of 170 mm with a packing density of 2.68 gm/cm^3. Three different probe liquids were used for contact angle measurements, diiodomethane, water, and formamide. Due to the high viscosity of glycerol, it was not used for column wicking. Hexane was used as a spreading liquid due to its low surface tension (78). It has been shown that for very low energy liquids θ equals zero (75), giving $\cos\theta = 1$. This facilitated calculation of R_e using hexane. For measuring the height of the liquid front with time, one end of the glass columns were immersed 5 mm (12) into the different liquids while holding the columns vertical. The time taken the liquid-front to rise every 4-mm was recorded discarding the first few readings due to possible initial disturbances (75). The slope of the straight-line plot of h^2 Vs t, going through the origin was used to calculate contact angles using equation 23. The procedure was repeated 5 times and the average contact angle was recorded.

For zeta potential measurement, oven dried ZVI was first sieved through a 45 μm sieve. The sieved material was then suspended in deoxygenated DI water in anaerobic chamber. The pH of the suspension was between 6.4-6.7. The suspension was allowed to sit 3 minutes to precipitate larger particles. Then the supernatant was collected and injected into the sample chamber and the ends of the chamber were capped. The sample chamber was then taken out of the anaerobic chamber and installed on the Lazer Zee Meter® for ζ-potential readings. A 3-minute equilibration time was allowed before taking the readings. ζ-potential of the ZVI was recorded as an average of 10 readings under an applied potential of 100 V.

E. PARTITIONING EXPERIMENT

For partitioning experiments, SRB cells were harvested at different physiological states following same procedure as described earlier. The harvested cells were suspended to the same volume as they were collected from using deoxygenated sterile DI water inside an anaerobic chamber. Approximate numbers of bacteria in the suspensions were determined as described before and dry weights of the suspensions were determined by drying the samples in a 105°C oven for 24 hours. The ZVI was oven dried at 105°C for 24 hours and sieved through a 106 μm sieve. Partitioning experiments were done in 40-mL vials with Teflon-lined screw caps. 20 mL of the cell suspension and 20 mg sieved ZVI were combined in each vial. Two sets of controls were included: 1 mg/mL sieved ZVI in deoxygenated sterile DI water and cell suspension without ZVI. Initial OD_{660} of the control with only cell suspension was measured. All vials were shaken in a rotary shaker at 80 rpm and at room temperature for 30 minutes. The contents of the vials were then filtered through MSI® 25-mm nylon filters of 5 μm size and the OD_{660} values were measured. Each experiment including controls were repeated five times and average readings recorded. OD_{660} reductions were calculated as a percent of the initial OD_{660}, i.e. the OD_{660} value of the filtrate from control with only cell suspensions.

SECTION III
QUALITY ASSURANCE AND QUALITY CHECK

A. PROJECT ORGANIZATION

The project team consisted of Dr. Strevett, Mr. Md. Shaheed, and Mr. Joe Grego. Dr. Strevett is the principal investigator (PI) and was responsible for the overall project. Md. Shaheed is a graduate research assistant and was responsible for running tests and analyzing results. Mr. Grego was a research associate of the Bioenvironmental Engineering and Science Laboratory and was responsible for the day-to-day operation of the analytical equipment. Each researcher was responsible for the QA/QC on their respective portion of the research.

B. ACCEPTANCE CRITERIA FOR DATA QUALITY

Laboratory methodologies were utilized to study and identify dominant microbial groups present in the soil cores. Initially, batch media screening methods were utilized. Full media analysis studies were used to evaluate the major microbial groups with the final goal to determine biofouling potential. Accuracy and repeatability of identification/enumeration studies were evaluated by analyzing replicates of select tube runs. Based on the overall objectives of this research, it was projected that data accuracy (and precision) within 5 to 10% would be sufficient.

C. DATA QUALITY NEEDS, ACCURACY, AND PRECISION

Data quality was important for analyzing the results of experiments designed to compare experimental variables. A laboratory quality assurance program is necessary to remove and reduce errors that may occur in our laboratory. Chemicals for media were ordered in quantities to last no longer than one year. When the media were prepared, manufacturer name, lot number, amount and appearance of media, date received, date opened and expiration date were logged. Precision was checked using duplicate analyses for each type sample examined. Duplicate runs conformed to a <10% frequency. Negative (sterile) controls for each series of samples were used to check sterility of the media and the dilution water. When sterile controls indicated contamination, samples affected were rejected and immediate re-sampling of those samples were performed. Positive control cultures were used to check media. Accuracy was assessed by comparison with samples of known bacterial concentration or identification. Analytical instruments (HPLC, spectrophotometers, contact angle meter, zeta-meter) were calibrated daily by running standards (e.g., three to five replicate injections for HPLC) at the beginning and end of each run and as necessary during a long run to establish calibration curves. If the standard deviation of the replicates was greater than an acceptable level (5%) the source of this variation was determined and necessary corrective actions were taken. Precision of chemical concentrations was also assessed (e.g., multiple injections on HPLCs and reporting of standard deviations). In terms of completeness, sufficient data were collected to allow sound scientific conclusions to be made (as discussed above).

D. SAMPLE HANDLING, PRESERVATION, AND STORAGE

Sample handling was detailed in the laboratory data book. Since the media characteristics of interest are the size distribution and mineral composition, these samples required anaerobic special handling or preservation considerations. Samples were stored in a cool (4°C), dry location where they were not affected by the chemicals utilized. Media stock samples were labeled by site, date of sampling, depth of sampling, and person(s) collecting the sample; this information was also included in the laboratory notebook. Aqueous samples were also stored in refrigerator (4°C) for subsequent analyses. Storage blanks were used as controls when storage was required.

E. QA/QC PRACTICES

Laboratory notebooks were maintained (in ink) for documenting the materials and methods utilized in this research, the experiments conducted (and the rationale for each experiment), observations made during the experiments, data collected, and data analysis.. Original data and summary data tables and figures were maintained in the laboratory notebook. Duplicate copies were maintained for all data stored on magnetic media (either a hard copy or a copy on separate magnetic media).

Analytical equipment had regularly scheduled maintenance and daily calibration (more frequent when appropriate). In the event that the variation in replicates of standards exceeded an acceptable level (~ 5%), the source of the variation was identified and the appropriate corrective action taken. An acceptance criteria of ~ 5% variation in three to five injections of standards was utilized with these standards injected at the beginning and end of HPLC runs (intermediate injections were also evaluated as warranted).

F. DATA REDUCTION, REPORTING AND ANALYSIS

Data reduction was conducted by computer spreadsheets (where appropriate) and recorded on hard copies and on magnetic media. This information was available to the project officer upon request. The information is presented in the final report by use of summary figures and tables in the text and appropriate appendix. Statistical analysis of data was conducted when appropriate (e.g., comparing means for differing treatments). In general, the focus of this research was major effects; however, statistical confidence in results was maintained.

G. QA REPORTS

Project reports included information on QA activities, when appropriate. Examples of information which appeared in the reports include the following: significant experimental problems encountered and corrective actions taken, major adjustments in experimental techniques and rationale, results of QA audits, significant adjustments in the project plan and recommended adjustments to the QA plan, etc.

SECTION IV
RESULTS AND DISCUSSION

A. MICROBIAL IDENTIFICATION AND ENUMERATION

SRB, ANA, and AER counts from upstream, reactive core ZVI, and downstream locations of the PRB are shown in Figure 1. SRB were the predominant group of microorganisms in ZVI and their numbers were approximately 2 to 4 orders of magnitude higher than in upstream and downstream locations. This result is supported by the findings of Liang et al. (35) who detected SRB in ground water and ZVI samples from a TCE contaminated site. ANA count was similar in the upstream and downstream samples. However, in ZVI, ANA count was approximately 2 orders of magnitude lower. AER count was lower than SRB and ANA at upstream and reactive core locations. AER were not detected at downstream location. No viable IRB or NO_3^--reducing microorganisms were detected in any of the samples.

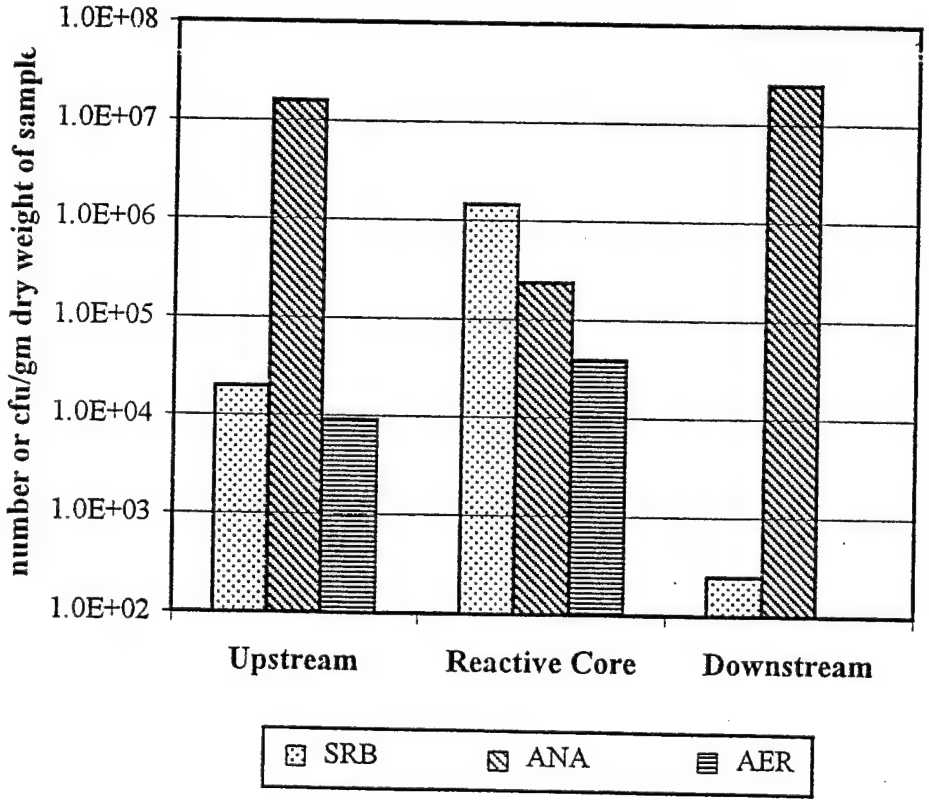

Figure 1. SRB, ANA, and AER Counts in Upstream, Reactive Permeable Core, and Downstream Locations of the PRB at DAFB.

Subsurface chemistry showed an oxidation-reduction potential (ORP) around -300 mV and dissolved oxygen (DO) concentration around 0.30 mg/L in ground water samples collected from the reactive core at DAFB*. This ORP is suitable for the proliferation of different anaerobic microorganisms, especially SRB and IRB (32, 80). Thus, our finding that SRB are the

* O'Sullivan, D., Personal communications; Tyndall Air Force Base, FL.

predominant organisms in the ZVI is in accordance with the subsurface redox chemistry at the site. SRB are an important group of morphologically closely related anaerobic microorganisms which have been shown capable of dehalogenation of different chlorinated solvents including TCE, PCE, DCE and also degradation of petroleum BTEX compounds by various researchers (7, 9, 10). SRB reduce subsurface sulfate and other sulfur compounds to sulfide, which can be coupled to oxidation of the ZVI forming iron sulfide mineral. Gu et al. recently reported microbially mediated iron-sulfide precipitate in ZVI columns (25). Liang et al. (35) also reported cementation of ZVI in their experimental columns as a possible result of iron-sulfide and other precipitates. Higher counts of SRB in the reactive zone compared to upstream and downstream locations, therefore, indicate that the actual degradation of the contaminants is possibly coupled to microbial sulfate reduction in the reactive zone. In that case, iron-sulfide precipitate could cause clogging problem of the permeable barrier at DAFB site.

Since ANA population at the upstream sampled location is very high, ANA have potential to be transported to the reactive core. However, once they reach the reactive core they have to compete with SRB, which are already the dominant populations within the reactive zone. AER count in the ZVI is around two orders of magnitude lower than the SRB and one order of magnitude lower than the ANA. This result is expected because of low DO values in the reactive zone *.

B. SURFACE TENSION PARAMETERS AND SURFACE POTENTIALS

1. Biotic Surfaces

Contact angle measurements and various surface thermodynamic characteristics of ZVI and SRB, ANA, and AER at different physiological states are summarized in Table 1. ζ–potentials measured for different groups of bacteria at different physiological states varied between –11.5 (ANA at logarithmic state) to –21.3 (ANA at decay state). However, all measured values stayed within the range of <25 mV at which the equations for determining the EL components of ΔG_{1W1} and ΔG_{1W2} are valid (72). Grasso et al. (24) reported a stationary state ζ-potential value 40-50 percent higher than in logarithmic or decay states for a pure strain *of Pseudomonas aeruginosa* Olin. However, our results show no such variation of ζ–potential for any group of bacteria among their different physiological states. These results conform to the findings reported by Smets et al. (57) where the measured ζ-potentials for centrifuged cells of *Pseudomonas fluorescens* remained between -17.3 to –18.4 mV at all states.

The LW component of surface tension (γ^{LW}) did not show large variation (standard deviation 2.37) among different consortia at different physiological states. This result conformed to the findings reported by other researchers (24, 57). However, magnitudes of γ^{LW} for all consortia were consistently higher than that reported for pure strains of *Pseudomonas aeruginosa* Olin (24) and *Pseudomonas fluorescens* (57). Lowest γ^{LW} (40.61 mJ/m^2) was observed for SRB at

* O'Sullivan, D., Personal communications; Tyndall Air Force Base, FL.

TABLE 1. SURFACE THERMODYNAMIC CHARACTERISTICS OF ZVI AND DIFFERENT GROUPS OF MICROORGANISMS AT DIFFERENT PHYSIOLOGICAL STATES

	Physiological State	Contact Angles (degrees)				ζ (mV)	Surface Tension Components (mJ/m^2)					ΔG_{1W1}^{TOT} (kT)
		Diiodomethane	glycerol	water	formamide		γ^{LW}	γ^{+}	γ^{-}	γ^{AB}	γ^{LW+AB}	
SRB	log	28	76	24	29	-20.2	45.03	6.62	25.17	25.81	70.84	-1710.6
	stationary	38	76	25	26	-18.2	40.61	5.35	30.67	25.60	66.21	4072.7
	decay	24	68	24	31	-19.3	46.51	3.58	31.33	21.17	67.68	4760.5
ANA	log	36	32	28	20	-11.5	41.57	1.34	41.67	14.94	56.51	19053.8
	stationary	25	32	22	20	-20.9	46.16	0.61	46.35	10.60	56.76	26408.6
	decay	38	40	24	36	-21.3	40.61	0.44	52.38	9.61	50.22	35043.5
AER	log	37	76	19	22	-18.2	41.09	5.95	32.02	27.60	68.69	4954.0
	stationary	34	79	23	30	-14.8	42.49	7.53	25.73	27.84	70.33	-1137.7
	decay	30	71	17	22	-17.5	44.23	4.67	33.56	25.02	69.25	6561.2
ZVI		77	*	70	60	-12.1	19.02	2.47	16.87	12.92	31.94	**

* Not measured

** Not calculated

stationary state and the highest γ^{LW} (46.51 mJ/m^2) was observed for the same at decay state. At all physiological states, the electron acceptor surface tension parameter (γ^-) were >28.5 mJ/m^2. Thus, ANA exhibited a monopolar hydrophilic surface (72, 74) at all states. However, for SRB and AER, γ^+ values were much greater than 1 mJ/m^2 and γ^- values were within 25.17 to 33.56 mJ/M^2 at all physiological states. Thus, SRB and AER did not show a dmoninant monopolar surface characteristic at any state.

2. Abiotic Surfaces

ZVI had a relatively low γ^{LW} value (Table 1). The γ^+ value of 2.47 mJ/m^2 and γ^- value of 16.87 mJ/m^2 showed that the ZVI surface was not monopolar (72, 74). The measured ζ–potential of ZVI (-12.1 mV) was within moderate range of <25-mV (72). However, magnitude of measured ζ–potential is dependent on ionic concentration of the liquid in which it is measured (50, 51). Thus, the ζ–potential value is not directly comparable with published ζ–potentials of other subsurface minerals (58) used for bacterial adhesion experiments.

C. HYDROPHOBICITY/HYDROPHILICITY OF MICROORGANISMS

Negative values of ΔG_{1W1} were obtained only for SRB at logarithmic state and for AER at stationary state (Table 1). Thus, only SRB at logarithmic state and AER at stationary state manifested hydrophobic cell surface characteristics. According to some researchers (24) this result also indicates more adhesion potential of the cells to another hydrophobic surface. In all other cases, ΔG_{1W1} were positive, indicating hydrophilicity of the cells. As the SRB cells went from logarithmic to stationary state, their cell surface characteristic changed from hydrophobic to hydrophilic. The cells became more hydrophilic from stationary to decay states. ANA cells also showed somewhat similar trend, where the cells became more hydrophilic as they went from logarithmic to stationary and from stationary to decay state. However, AER cells became hydrophilic to hydrophobic as they went from logarithmic to stationary state. The cells became hydrophilic again as they entered decay state. Hydrophilicity of AER cells in decay state was more than in logarithmic state.

Highest hydrophobicity of SRB, ANA, and AER were not observed at the same physiological state. This result is supported by the findings reported by different researchers. Grasso et al. (24), Smets et al. (57), Allison et al. (1), and Dufrêne and Rouxhet (16) reported increases in cell hydrophobicity from logarithmic to stationary state for *Pseudomonas aeruginosa* Olin, Pseudomonas fluorescens, *Escherichia coli*, and *Azospirillium brasilense,* respectively. van Loosdrecht et al. (65, 67) and Wrangstadh et al. (81) reported increases in cell hydrophobicity from a logarithmic state for different bacterial strains under examination. McEldowney and Fletcher (42), on the contrary, observed no change in bacterial cell surface hydrophobicity among different physiological states. Our results show that SRB and AER exhibited highest hydrophobicity in logarithmic and stationary states, respectively. ANA cells remained hydrophilic at all states with decreasing hydrophilicity from decay to stationary to logarithmic states. Since bacterial cell-surface characteristics vary widely among different bacteria (55), it is no surprise that there is no fixed physiological state at which all bacteria would show highest or lowest hydrophobicity.

D. INTERACTION OF CELLS WITH ZERO VALENT IRON

The ExDLVO plots of the total interaction energy between ZVI and different groups of bacteria at different physiological states are shown in Figures 2, 3, and 4. For SRB at small separation distances (approximately <10 Å), the AB forces dominated (Figures A-1, A-2, and A-3) and the cells showed negative ΔG_{1W2} values at all physiological states (Figure 2). In logarithmic state, highest negative free energy was observed. Magnitude of ΔG_{1W2}^{TOT} in stationary state was the lowest but similar to the magnitude of ΔG_{1W2}^{TOT} at decay state. This indicated highest adhesion potential of SRB cells to ZVI surface at logarithmic state and lowest potential for adhesion at stationary state. The ΔG_{1W2}^{TOT}-values for ANA remained positive at all separation distances and at all physiological states (Figure 3). At small separation distances, AB forces dominated (Figures A-4, A-5, and A-6) and the magnitude of ΔG_{1W2}^{TOT} increased as the cells went from logarithmic to stationary and from stationary to decay states. Thus, ANA showed decreasing adhesion potential to ZVI surface as the cells went from logarithmic to stationary and from stationary to decay states. For AER at short distances, highest negative free energy was observed for cells in stationary state (Figure 4), where AB forces dominated (Figure A-8). In logarithmic and decay states, the AB forces were mostly balanced out by LW forces and the shape of ΔG_{1W2}^{TOT} curve was dominated by EL forces (Figures A-7 and A-9). AER showed highest adhesion potential to ZVI surface at stationary state and lowest at decay state. Because decays of LW and EL forces were very rapid (Figures A-7, A-8, and A-9), at larger separation distances (approximately >25 Å) the EL forces dominated for all consortia at all physiological states. Thus, at large separation distances SRB, ANA, and AER showed very gradual decay of G_{1W2}^{TOT} at all physiological states.

The observed ΔG_{1W2}^{TOT} variation with distance (Figures 2, 3, and 4) describes the adhesion potential of SRB, ANA, and AER to ZVI surface. At small separation distances, SRB showed large favorable energy for adhesion, whereas, ANA showed high-energy barrier to adhesion at all physiological states. On the contrary, at small separation distances, behavior of AER varied among different states, where the cells showed large favorable energy for adhesion at only stationary state. Comparatively low favorable energy of adhesion was observed at logarithmic state and an energy barrier for adhesion existed at decay state.

Although ΔG_{1W2}^{TOT} varied among different physiological states for all groups of microorganisms at small separation distances, at larger distances their behavior was very similar. At larger separation distances, the microorganisms showed a very gradually decaying energy barrier to adhesion. This result was expected since the EL component of ΔG_{1W2}^{TOT} dominated at larger separation distances. Shape of the EL component curve is dependent on the ionic strength of the liquid medium. At higher ionic strengths (around 0.1-0.01 M) decay of EL component is very sharp (72). As the ionic strength is lower, the decay of EL becomes increasingly gradual. Since the DI, water used in our experiments was of negligible ionic strength, the decay with distance of the EL component and ultimately ΔG_{1W2}^{TOT} was very gradual. Limited data available from actual field measurements* suggests relatively high ionic strength of the ground water collected from the reactive core. An increase in ionic strength would have resulted in a sharp

* O'Sullivan, D., Personal communications; Tyndall Air Force Base, FL.

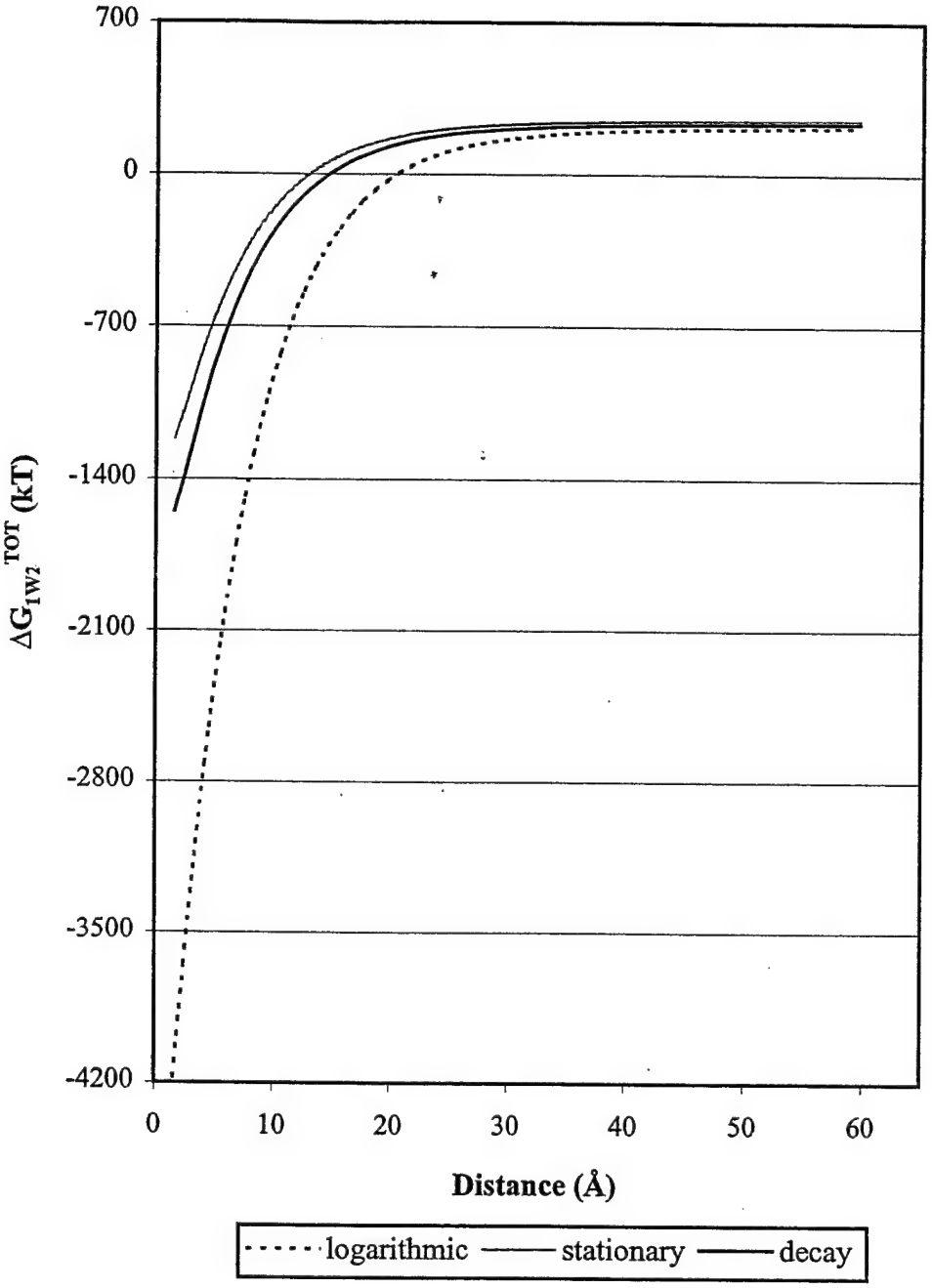

Figure 2. Variation of Total Interaction Energy Between ZVI and Bacterial Cells, ΔG_{1W2}^{TOT} (kT) with Distance (Å) for SRB at Logarithmic Growth, Stationary, and Decay States.

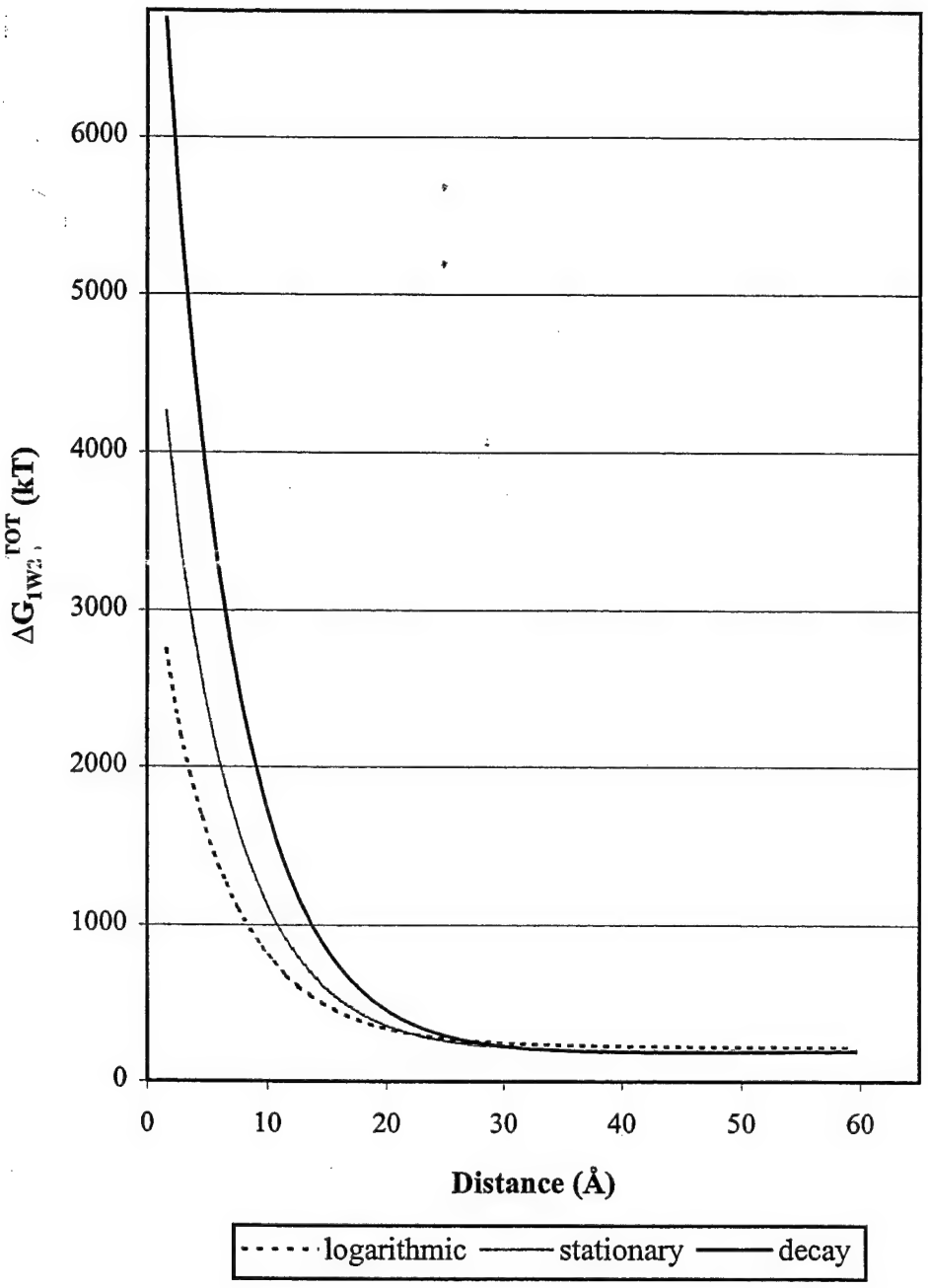

Figure 3. Variation of Total Interaction Energy Between ZVI and Bacterial Cells, ΔG_{1W2}^{TOT} (kT) with Distance (Å) for ANA at Logarithmic Growth, Stationary, and Decay States.

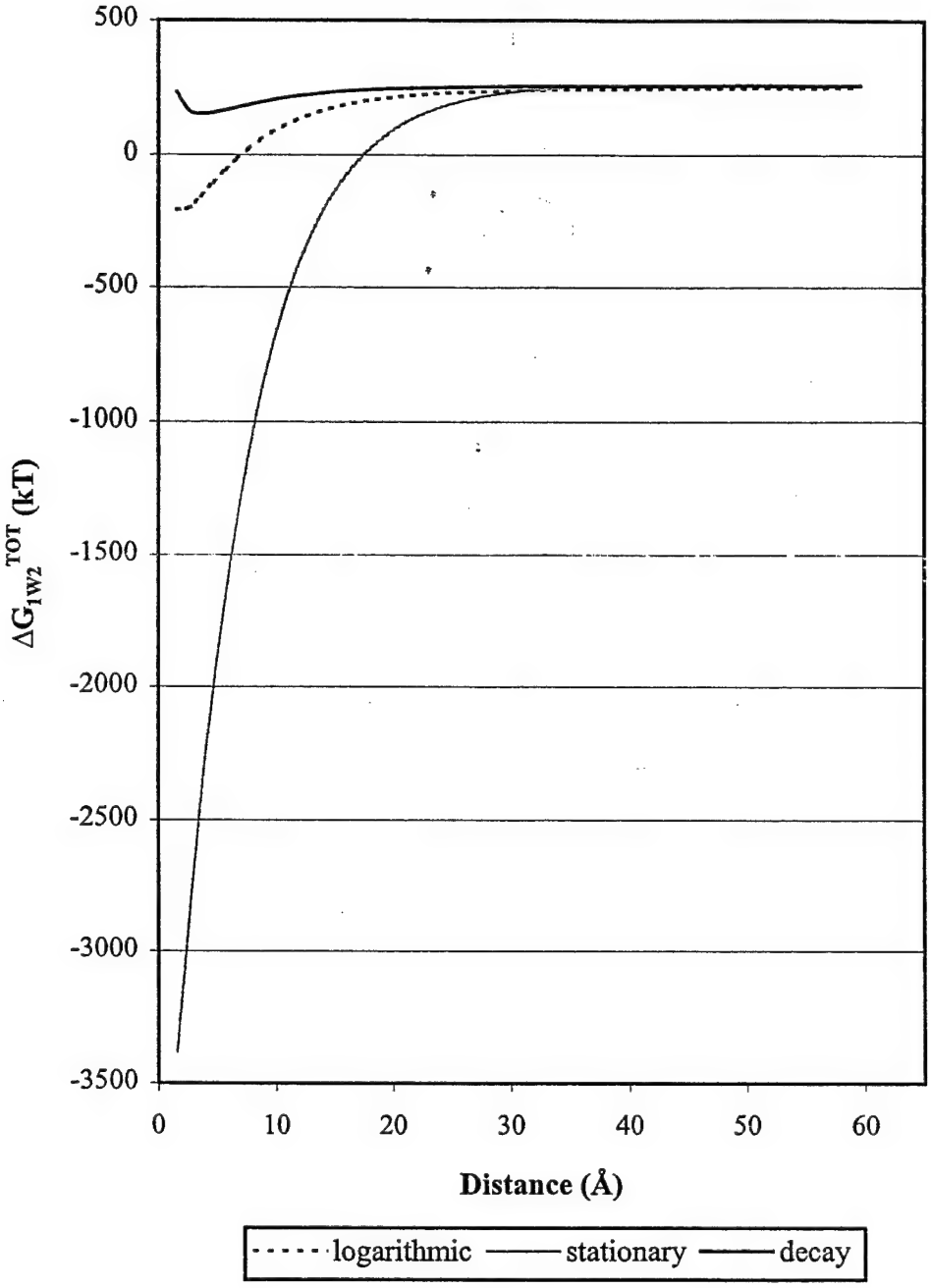

Figure 4. Variation of Total Interaction Energy Between ZVI and Bacterial Cells, ΔG_{1W2}^{TOT} (kT) with Distance (Å) for AER at Logarithmic Growth, Stationary, and Decay States.

decrease in the EL component. However, in most cases, AB component dominated and small variation in EL component would not produce significant affect on the shapes and magnitudes of the ΔG_{1W2}^{TOT} curves. Thus, our results are adequate for describing adhesion potentials of the different groups of microorganisms at their different physiological states.

An interesting behavior of SRB, the dominant group of microorganisms in the reactive core, is worth noticing. SRB cells showed highest hydrophobicity (indicated by ΔG_{1W1}^{TOT} calculations) and correspondingly the highest adhesion potential (indicated by ΔG_{1W2}^{TOT} calculations) at logarithmic state. However, although the cells at decay state were more hydrophilic than cells at stationary state, at short distances decay state cells showed more adhesion potential to ZVI compared to cells in stationary state. This result is contrary to the reports of a number of authors, who described surface hydrophobicity/hydrophilicity as the only measure for adhesion of cell to surfaces (24, 58, 65). To validate the theoretical observations, subsequent partitioning experiments were conducted.

E. PARTITIONING EXPERIMENT

Partitioning of SRB at different physiological states between suspended and attached to ZVI phases was measured as a percent reduction of OD_{660} (Table 2). The controls with only cell suspensions showed no change in OD_{660}, confirming the recovery of all the bacteria after filtration. The filtrate of the control with ZVI in DI water showed consistent OD_{660} of 0.01, which was possibly due to dislodgment of some originally present microorganisms from the ZVI. This value was considered as a background concentration and was subtracted from OD_{660} readings of the filtrates to get the actual OD_{660} reading of the introduced cells in filtrate. Highest partitioning (26.5%) was observed at logarithmic state. At stationary state, partitioning of bacteria was lowest (14.1%) and was almost half of that at logarithmic state. Decay state partitioning (17.0%) was closer to but higher than that at stationary state. The results also showed greater partitioning of cells at decay state compared to the cells at stationary state. Consequently, our experimental observations were consistent with the theoretical predictions of adhesion potentials through ΔG_{1W2}^{TOT} calculations. A few other researchers also report similar observations (57, 70). Thus, ΔG_{1W2}^{TOT} can provide satisfactory prediction for adhesion potential of groups of microorganisms to ZVI. The results from the partitioning experiments confirmed the predicted adhesion of SRB to ZVI by the XDLVO calculations.

TABLE 2. PARTITIONING RESULTS FOR SRB AT DIFFERENT PHYSIOLOGICAL STATES

Physiological State	Initial Concentration		Initial OD_{660}	% Reduction of OD_{660}
	number/mL	dry wt./mL		
log	3.25×10^6	0.130	0.113	26.5
stationary	5.0×10^6	0.146	0.128	14.1
decay	8.0×10^6	0.270	0.224	17.0

SECTION V
CONCLUSIONS

The few PRB long-term performance studies mostly focused on the chemical aspect of the reactive core. The observed flow reductions and performance deterioration typically was postulated as a result of chemical precipitation. Although biofouling was observed in Newbury Park, CA (53) and Portsmouth, OH (35), a model for predicting the potential for such biofouling in PRBs was not present. Our study shows that the dominant SRB population at DAFB site permeable reactive core has the potential for biofouling, which can be predicted by bacterial surface thermodynamics approach. This report thus presents an optimal method for the prediction of biofouling potential and assessment of long-term microbiological performance of PRBs.

REFERENCES

1. Allison, D. G.; Brown, M. R. W.; Evans, D. E.; Gilbert, P., J. Bacteriol. 1990, 172, 1667.
2. American Public Health Association (APHA), Standard Methods for the Examination of Water and Wastewater, 18th ed.; American Public Health Association, American Water Works Association, and Water Environment Federation: Washington D. C., 1992, 9-36.
3. Anderson, L. D.; Kent, D. B.; Davis, J. A., Environ. Sci. Technol. 1994, 28, 178-185.
4. Atlas, R. M., Media for Environmental Microbiology; CRC Press: New York, 1995.
5. Bellin, C. A.; Rao, P. S. C., Appl. Environ. Microbiol. 1993, 59, 1813-1820.
6. Benner, S. G.; Blowes, D. W.; Gould, W. D.; Herbert, R. B. Jr.; Ptacek, C. J., Environ. Sci. Technol. 1999, 33, 2793-2799.
7. Boyle, A. W.; Phelps, C. D.; Young, L. Y., Appl. Env. Microbiol. 1999, 65, 1133-1140.
8. Busscher, H. J.; Weerkamp, A. H.; van der Mei, H. C.; van Pelt, A. W. J.; de Jong, H. P.; Arends, J., Appl. Env. Microbiol. 1984, 48, 980-983.
9. Cabirol, N.; Jacob, F.; Perrier, J.; Fouillet, B.; Chambon, P., J. Gen. Appl. Microbiol. 1998, 44, 297-301.
10. Chen, C. I.; Taylor, R. T., Appl. Microbiol. Biotech. 1997, 48, 121-128.
11. Cochran, W. G., Biometrics. 1950, 6, 105-116.
12. Costanzo, P. M.; Giese, R. F.; van Oss, C. J., Langmuir. 1995, 11, 1827-1830.
13. Denyer, S.P.; Hanlon, G.W.; Davies, M. C., *In:* Microbial Biofilms: Formation and Control, Eds. Denyer, S. P.; Gorman, S. P.; Sussman, M., Blackwell Scientific Publications, Boston, 1993, pp. 13-27.
14. Derjaguin, B. V.; Landau, L. D., Acta Physiochim. USSR 1941, 14, 633.
15. Drozd, C.; Schwartzbrod, J., Appl. Env. Microbiol. 1996, 62, 1227-1232.
16. Dufrêne, Y. F.; Rouxhet, P. G., Can. J. Microbiol. 1996, 42, 548.
17. Farrell, J.; Kason, M.; Melitas, N.; Li, T., Environ. Sci. Technol. 2000, 34, 514-521.
18. Fattom, A.; Shilo, M., Appl. Environ. Microbiol. 1984, 47, 135-143.
19. Fruchter, J. S.; Cole, C. R.; Williams, M. D.; Vermeul, V. R.; Amonette, J. E.; Szecsody, J. E.; Istok, J. D.; Humphrev, M. D., Ground Water Monit. Rem. 2000, 20, 66-78.
20. Gannon, J. T.; Manilal, V. B.; Alexander, M., Appl. Environ. Microbiol. 1991, 57, 190-193.
21. Gannon, J., T.; Baveye, P.; Alexander, M., Appl. Environ. Microbiol. 1991, 57, 2497-2501.
22. Gerba, C.P., *In:* Groundwater Quality, Eds. Ward, C.H.; Giger, W.; McCarty, P.L., John Wiley and Sons, New York, 1985, pp.53-67.
23. Ghiorse, W. C., *In:* Methods of Soil Analysis: Microbiological and Biochemical Properties, Eds. Weaver, R. W.; Angle, S.; Bottomley, P.; Bezdicek, D.; Smith, S.; Tabatabai, A.; Wollum, A., Soil Science Society of America Book Series, 1994, 5, 1081-1094.
24. Grasso, D.; Smets, B. F.; Strevett, K. A.; Machinist, B. D.; van Oss, C. J.; Giese, R. F.; Wu, W., Environ. Sci. Technol. 1996, 30, 3604-3608.
25. Gu, B.; Phelps, T. J.; Liang, L.; Dickey, M. J.; Roh, Y.; Kinsall, B. L.; Palumbo, A. V.; Jacobs, G. K., Environ. Sci. Technol. 1999, 33, 2170-2177.
26. Hamaker, H. C., Physica. 1937, 4, 1058.
27. Harkness, M. R.; Bracco, A. A.; Brennan, M. J.; Deweerd, K. A., Environ. Sci. Technol. 1999, 33, 1100-1109.

28. Hiemenz, P. C.; Rajagopalan, R., Principles of Colloid and Surface Chemistry, Marcel Dekker, Inc., New York, 1997.
29. Israelachvili, J. N., Intermolecular and Surface Forces, Academic Press, New York, 1992.
30. Jang, L. K.; Chang, P. W.; Findley, J. E.; Yen, T. F., Appl. Environ. Microbiol. 1983, 46, 1066-1072.
31. Jenkins, M.; Lion, L.W., Appl. Environ. Microbiol. 1993, 59, 3306-3313.
32. Jones, J. G., *In:* Sediment Microbiology, Eds. Nedwell, D. B.; Broun, C. M.,, Academic Press, New York, 1982, 107-145.
33. Li, Z.; Jones, H. K.; Bowman, R. S.; Helforich, R., Environ. Sci. Technol. 1999, 33, 4326-4330.
34. Liang, L.; Korte, N.; Goodlaxson, J. D.; Clausen, J.; Fernando, Q.; Mufrikia, R., Ground Water. Monit. Rem. 1997, 17, 122-127.
35. Liang, L.; West, O. R.; Korte, N. E.; Goodlaxson, J. D.; Pickering, D. A.; Zutman, J. L.; Anderson, F. J.; Welch, C. A.; Pelfrey, M. J.; Dickey, M. J., A field-scale test of trichloroethylene dechlorination using iron filings for the X-120/X-749 groundwater plume; ORNL/TM-13217, Oak Ridge National Laboratory, Oak Ridge, TN, 1997.
36. Lindqvist, R.; Enfield, C. G., Appl. Environ.. Microbiol. 1992, 58, 2211-2218.
37. Lindqvist, R.; Bengtsson, G., Microb. Ecol. 1991, 21, 49-72.
38. Lindqvist, R.; Soo Cho, J.; Enfield, C., Wat. Resour. Res. 1994, 12, 3291-3299.
39. Loeb, G. I., *In:* Bacterial Adhesion, Eds. Savage, D. C.; Fletcher, M., Plenum Press, New York, 1985, pp. 111-129.
40. Marshall, K. C.; Stout, R.; Mitchell, R., J. Gen. Microbiol. 1971, 68, 337.
41. McDowell-Boyer, L. M.; Hunt, J. R. Sitar, N., Water Resour. Res. 1986, 22, 1901-1921.
42. McEldowney, S.; Fletcher, M., J. Gen. Microbiol. 1986, 132, 513-523.
43. Mills, A. L.; Herman, J. S.; Hornberger, G. M.; DeJesus, T. H., Appl. Environ. Microbiol. 1994, 60, 3300-3306.
44. Mozes, N.; Marchal, F.; Hermesse, M. P.; Van Haecht, J. L.; Reuliaux, L.; Leonard, A. J.; Rouxhet, P. G., Biotechnol. Bioeng. 1987, 30, 439-450.
45. O'Hannesin, S. F.; Gillham, R. W., Ground Water 1998, 36, 164-170.
46. Overbeek, J. T. G., *In:* Colloid Sci., Ed. Kruyt, H. R., 1952, 1, 144.
47. Postgate, J. R., Methods in Microbiology, 1969, 1, 611-628.
48. Righetti, P. G.; van Oss, C. J.; Vanderhoff, J. W., Eds. Electrokinetic Separation Methods, Elsevier, Amsterdam, 1979.
49. Rijnaarts, H. H. M.; Norde, W.; Bouwer E. J.; Lyklema J.; Zehnder A. J. B., Appl. Environ. Microbiol., 1993, 59, 3255-3265.
50. Rijnaarts, H. H. M.; Norde, W.; Bouwer, E. J.; Lyklema, J.; Zehnder, A. J. B., Colloids and Surf. B: Biointerfaces 1995, 4, 5-22.
51. Rijnaarts, H. H. M.; Norde, W.; Lyklema, J.; Zehnder, A. J. B. Colloids and Surf. B: Biointerfaces 1999, 14, 179-195.
52. Rouxhet, P. G.; Mozes, N., *In:* Anaerobic Digestion: Results of Research and Demonstration Projects, Eds. Ferranti, M. P.; Ferreo, G. L.; L'Hermite, P., Elsevier Applied Science, New York, 1987.
53. RTDF web site: HTTP://WWW.RTDF.ORG.
54. Rutter, P. R.; Vincent, B., *In:* Microbial Adhesion and Aggregation, Ed. Marshall, K. C., Springer-Verlag, New York, 1984, 21-38.

55. Sheytr, W. U.; Messner, P.; Miniken, D. E.; Heelds, V. E.; Vivji, M., *In:* Bacterial Cell Surface Techniques, Eds. Hancock, I.; Poxton, I., Wiley, New York, 1988, 1-30.
56. Site Characterization Work Plan for the Area 5 Funnel-and-Gate Demonstration Site, Dover Air Force Base, Delaware, Battelle, Columbus, Ohio,1997.
57. Smets, B. F.; Grasso, D.; Engwall, M. A.; Machinist, B. J., Colloids and Surf. B: Biointerfaces 1999, 14, 121-139.
58. Stenström, T. A., Appl. Env. Microbiol. 1989, 55, 142-147.
59. Tanner, R. S., Proceedings, The Fifth International Conference on Microbial Enhanced Oil Recovery and Related Biotechnology for Solving Environmental Problems, 1995, 353-362.
60. Taylor S.; Jaffé, P., Wat. Resour. Res. 1990, 26, 2181-2194.
61. Thomas, J. M., Ward, C. H., Environ. Sci. Tech. 1989, 23, 760-766.
62. Trevors, J. T.; van Elsas, J.; van Overbeek, L. S., Appl. Env. Microbiol. 1990, 56, 401.
63. United States Environmental Protection Agency; EPA/600/R-98/125, Office of Solid Waste and Emergency Response, Washington DC, 1998.
64. van Loosdrecht, M. C. M.; Lyklema, J.; Norde, D.; Schraa, G.; Zehnder, A. J. B., Appl. Env. Microbiol. 1987, 53, 1893-1897.
65. van Loosdrecht, M. C. M.; Lyklema, J.; Norde, D.; Schraa, G.; Zehnder, A. J. B., Appl. Env. Microbiol. 1987, 53, 1898-1901.
66. van Loosdrecht, M. C. M.; Lyklema, J.; Norde, D.; Zehnder, A. J. B., Microb. Ecol. 1989, 17, 1-15.
67. van Loosdrecht, M. C. M.; Norde, D.; Zehnder, A. J. B., *In:* Proceedings of the European Congress on Biotechnology, Eds. Neijssel, O. M.; van der Meer, R. R.; Luyben, K. C. A. M., Elsevier, Amsterdam, 1987.
68. van Loosdrecht, M. C. M.; Norde, D.; Zehnder, A. J. B., J. Biomaterials Applications. 1990, 5, 91-106.
69. van Loosdrecht, M. C. M.; Lyklema, J.; Norde, W.; and Zehnder, A. J. B., Microb. Rev., 1990, 54, 75-87.
70. van Oss, C. J., Biofouling 1991, 4, 25-35.
71. van Oss, C. J., *In:* Biophysics of the Cell Surface, Eds. Glaser R., Gingell, D., Springer-Verlag, New York, 1990, 131-152.
72. van Oss, C. J., Interfacial Forces in Aqueous Media, Marcel Dekker, Inc., New York, 1994.
73. van Oss, C. J.; Chaudhury, M. K.; Good, R. J., Chem. Rev. 1988, 88, 927-941.
74. van Oss, C. J.; Giese, R. F., Clays Clay Miner. 1995, 43, 474-477.
75. van Oss, C. J.; Giese, R. F.; Li, Z.; Murphy, K.; Norris, J.; Chaudhury, M. K.; Good, R. J. J., J. Adhesion Sci. Technol. 1992, 6, 413-428.
76. van Oss, C. J.; Good, R. J., Colloids Surfaces 1984, 8, 373.
77. Verwey, E. J. W.; Overbeek, J. Th. G., Trans. Faraday Soc., 1946, 42B, 117.
78. Wålinder, M. E. P.; Gardner, D. J., J. Adhesion Sci. Technol. 1999, 13, 1363-1374.
79. Washburn, E. W., Phys. Rev. 1921, 17, 273-283.
80. Watanabe, I.; Furusaka, C., Adv. Microb. Ecol. 1980, 40, 125-168.
81. Wrangstadh, M.; Conway, P. L.; Kjelleberg, S., Arch. Microbiol. 1986, 145, 220-227.
82. Wu, W.; Giese, R. F.; van Oss, C. J., Colloids and Surf. B: Biointerfaces 1999, 14, 47-55.
83. Yates, M. V.; Yates, S. R., Crit. Rev.Environ.Control 1988, 17, 304-344.
84. Zysset, A.; Stauffer, F.; Dracos, T., Wat. Resour. Res. 1994, 30, 2423-2434.

APPENDIX A
TOTAL INTERACTION ENERGY AND ITS COMPONENTS

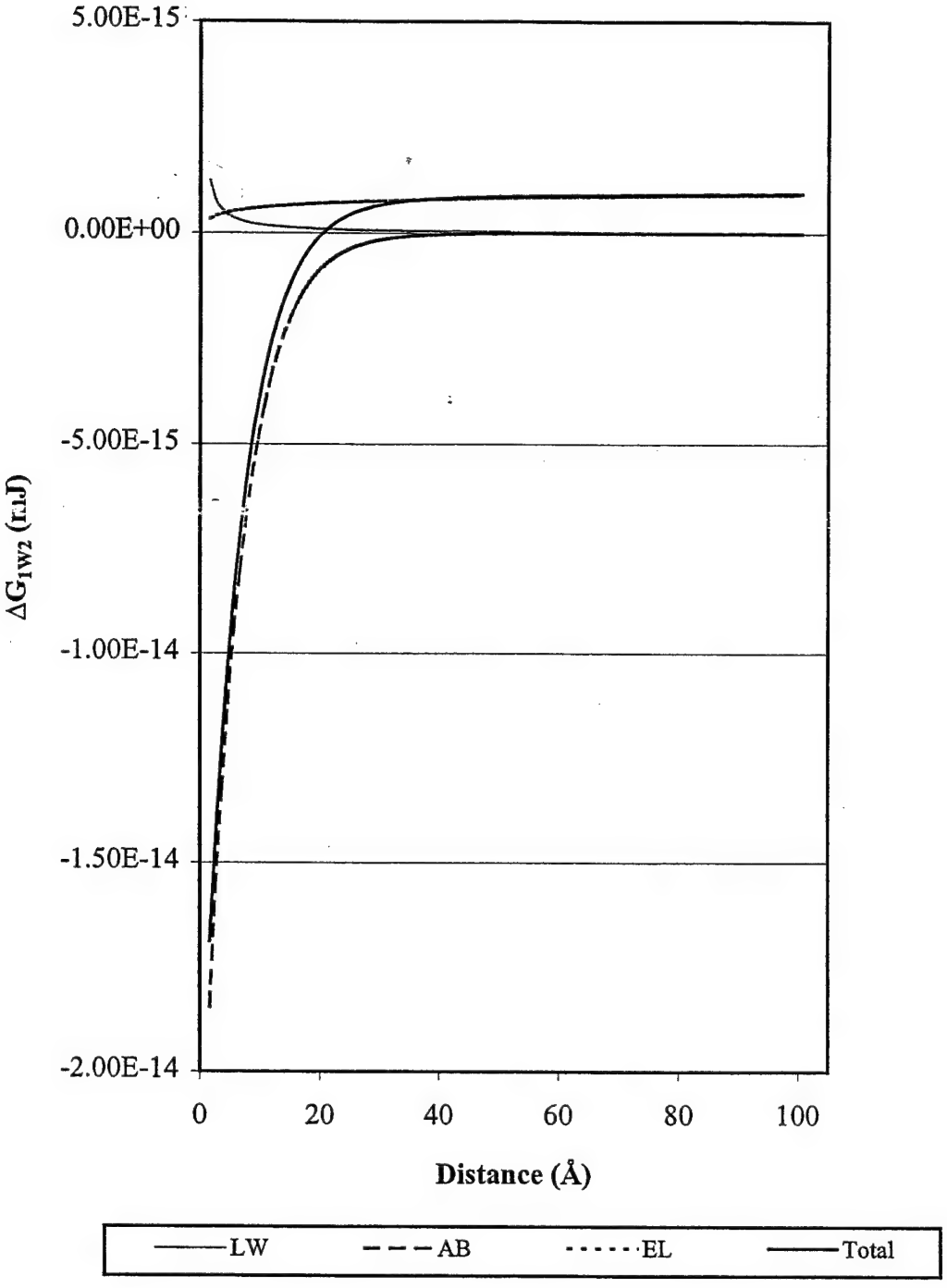

Figure A-1. Variation of Total Interaction Energy and Its Components with Distance Between ZVI and SRB at Logarithmic Growth State.

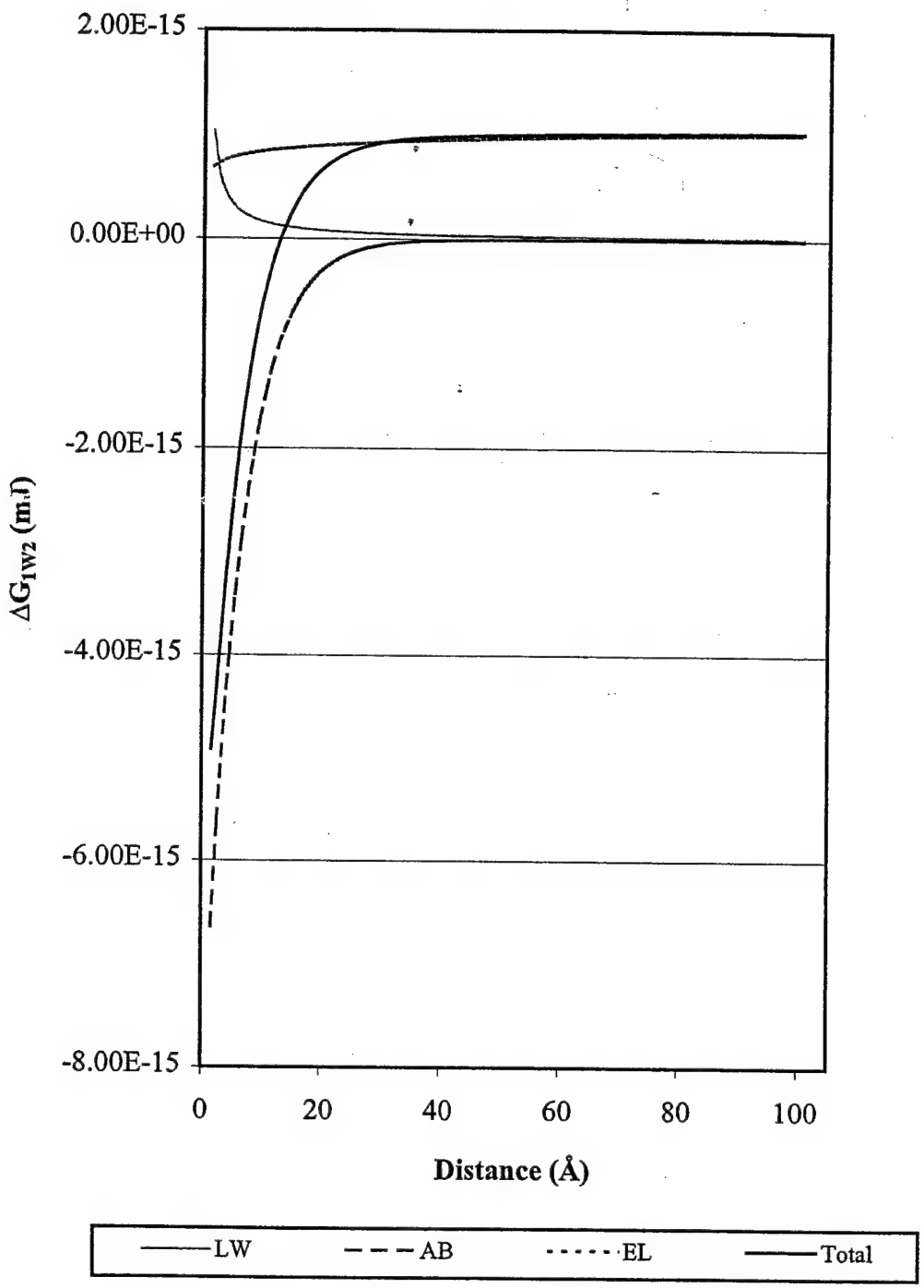

Figure A-2. Variation of Total Interaction Energy and Its Components with Distance Between ZVI and SRB at Stationary State.

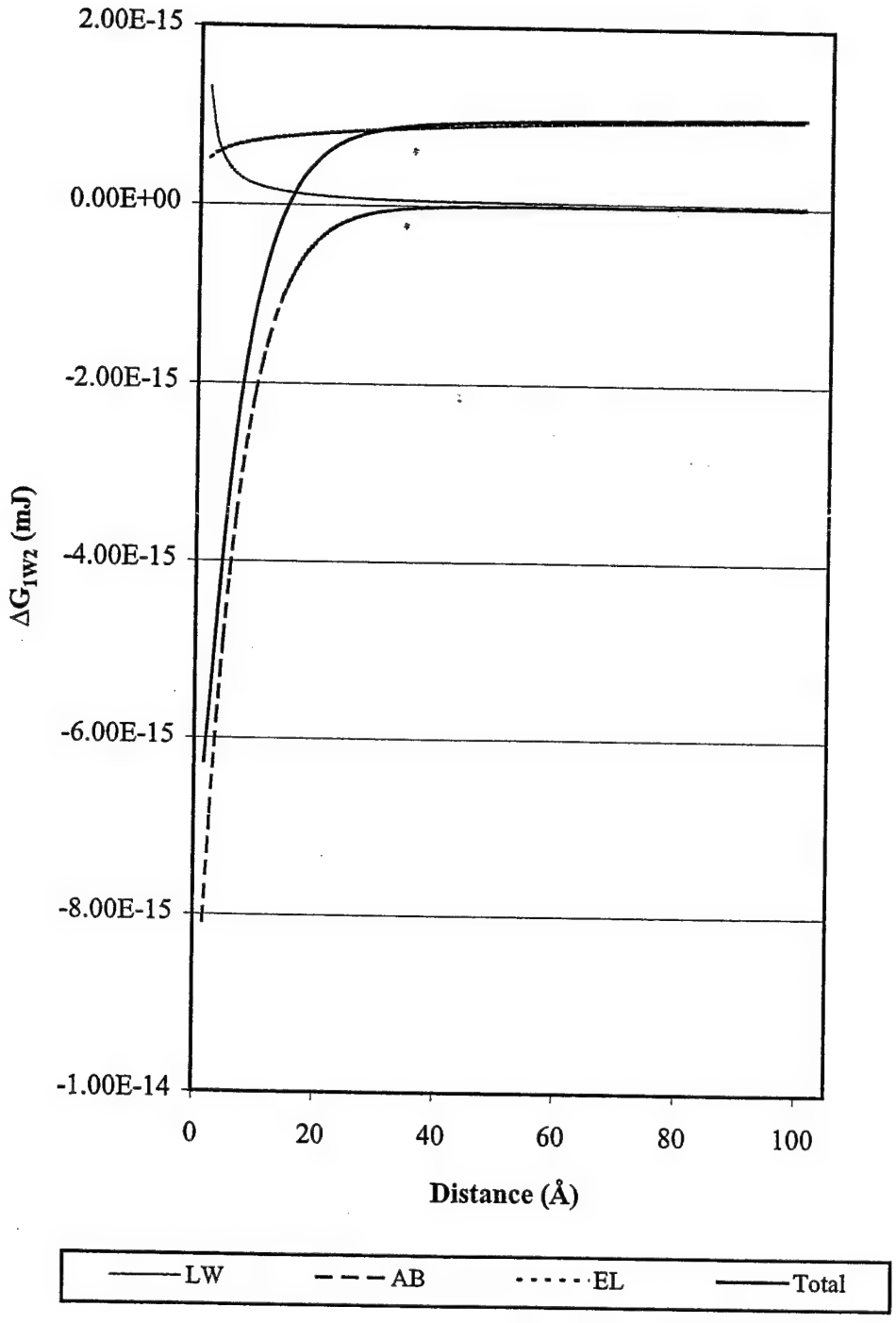

Figure A-3. Variation of Total Interaction Energy and Its Components with Distance Between ZVI and SRB at Decay State.

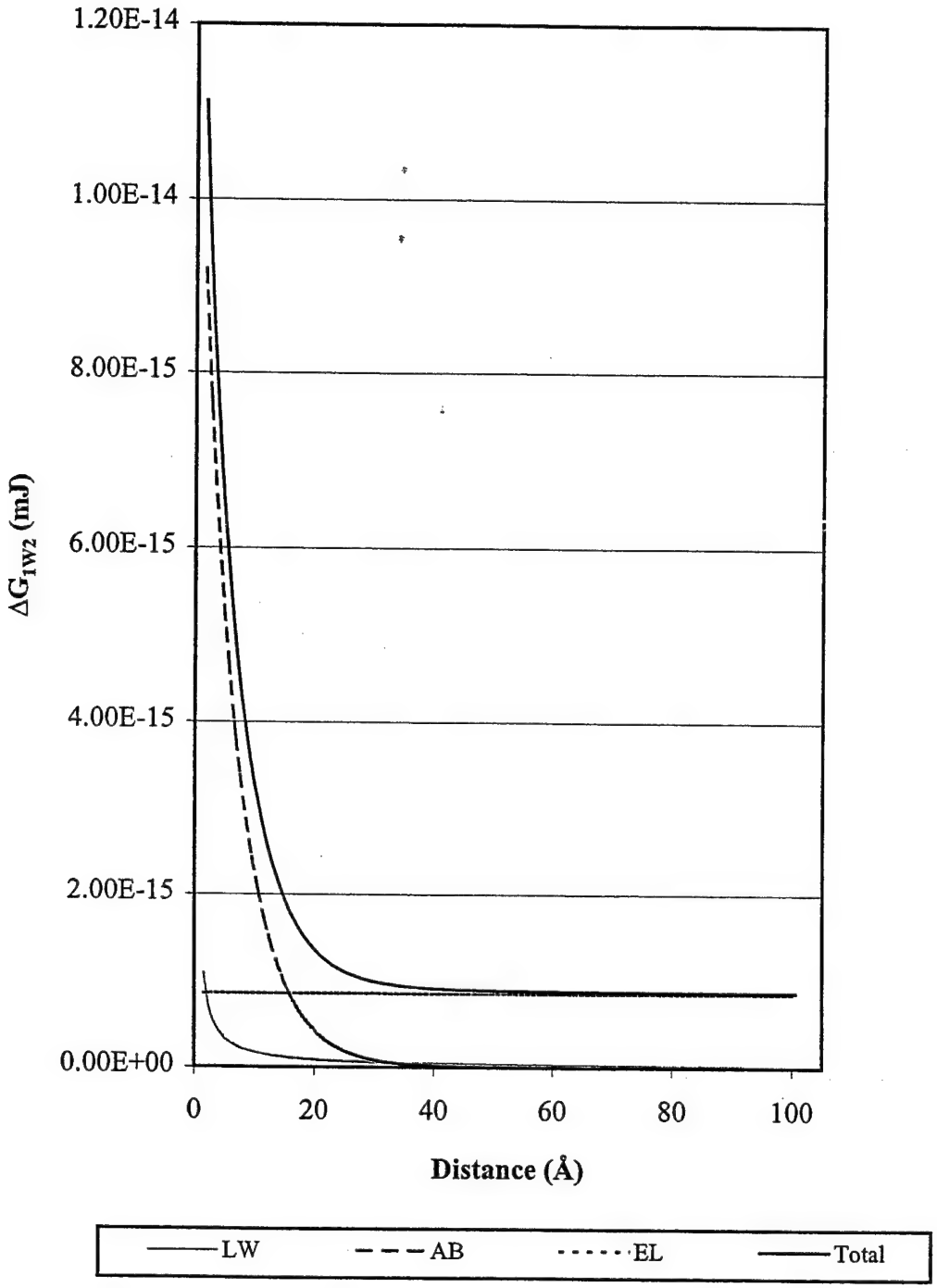

Figure A-4. Variation of Total Interaction Energy and Its Components with Distance Between ZVI and ANA at Logarithmic Growth State.

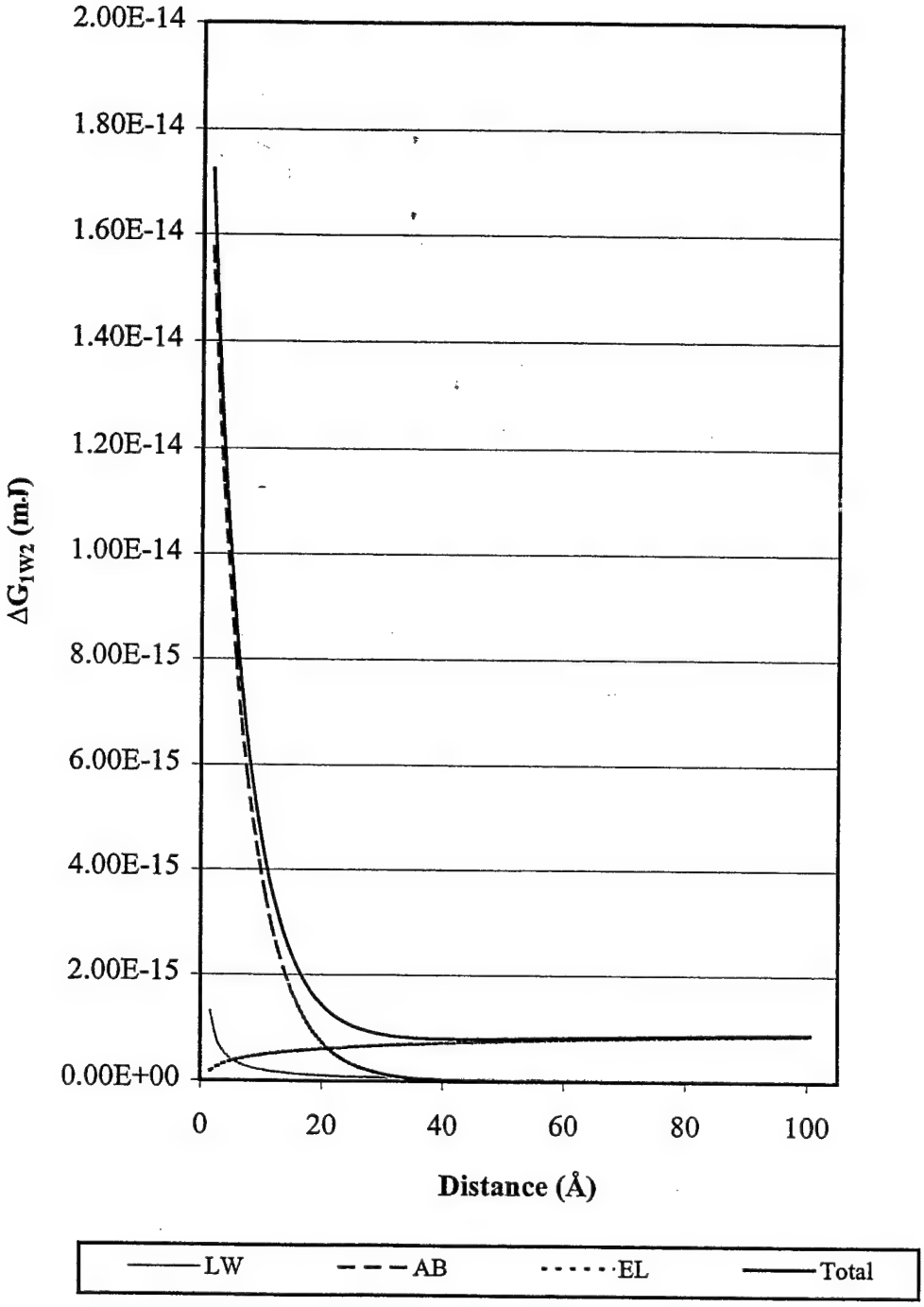

Figure A-5. Variation of Total Interaction Energy and Its Components with Distance Between ZVI and ANA at Stationary State.

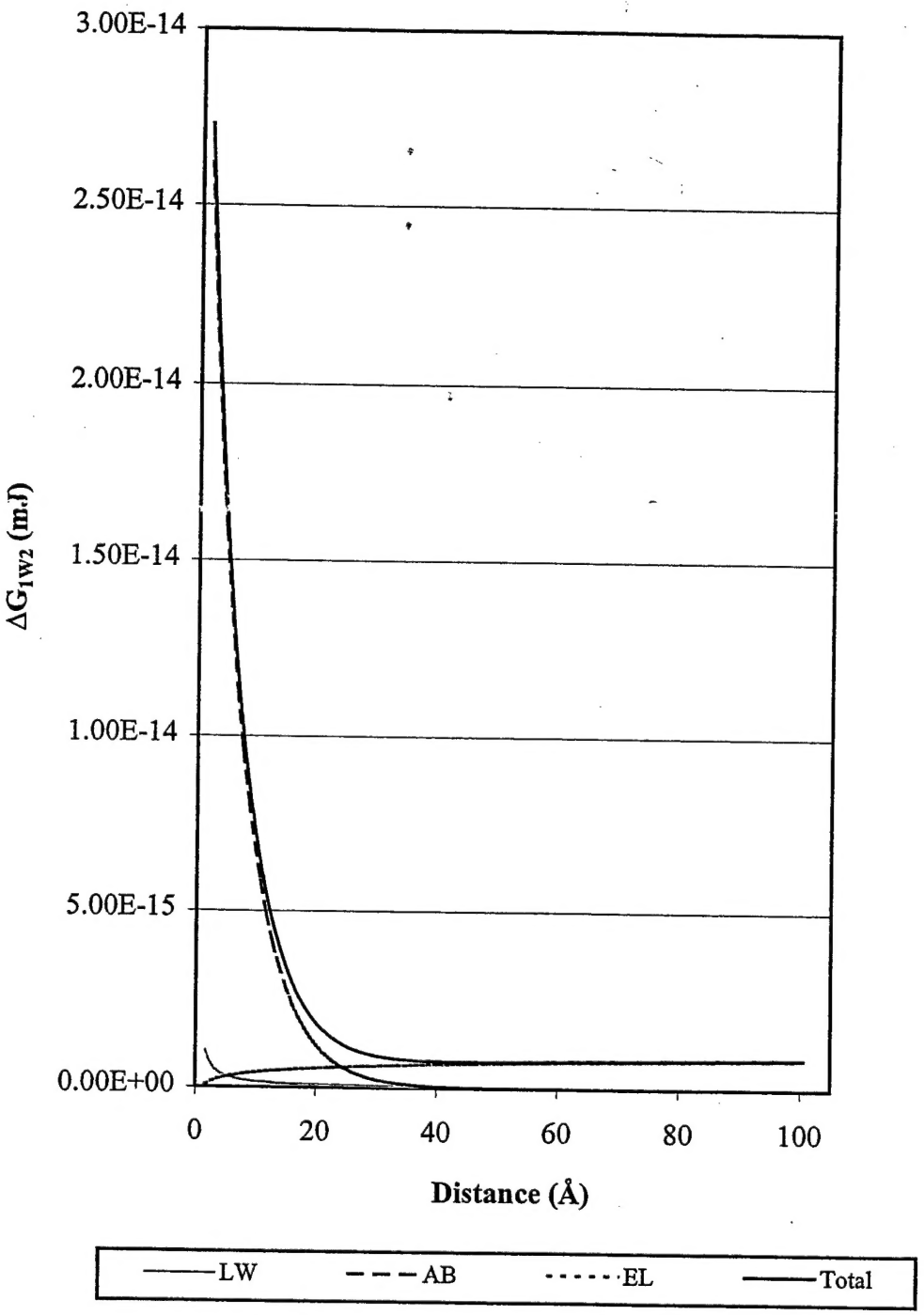

Figure A-6. Variation of Total Interaction Energy and Its Components with Distance Between ZVI and ANA at Decay State.

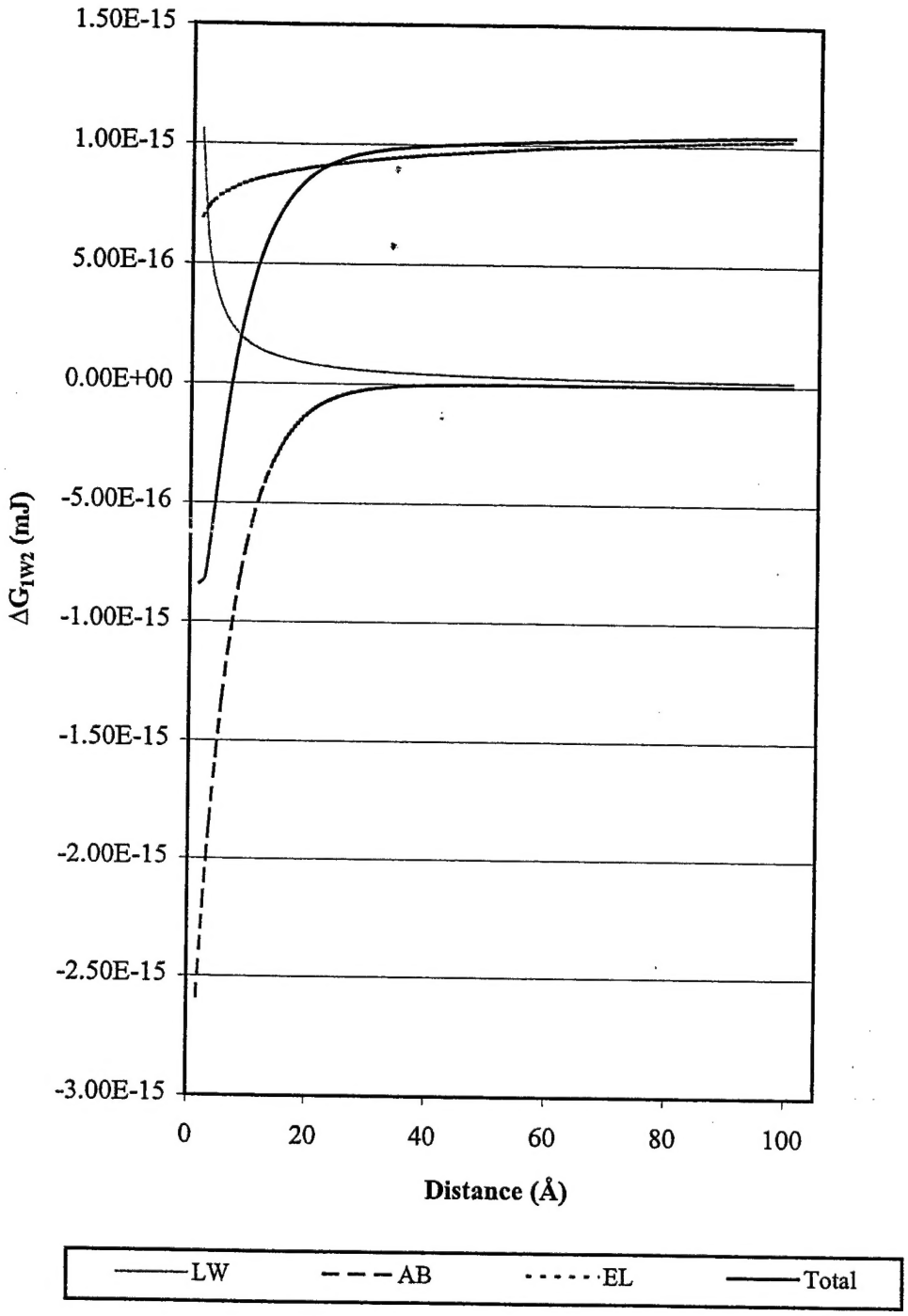

Figure A-7. Variation of Total Interaction Energy and Its Components with Distance Between ZVI and AER at Logarithmic Growth State.

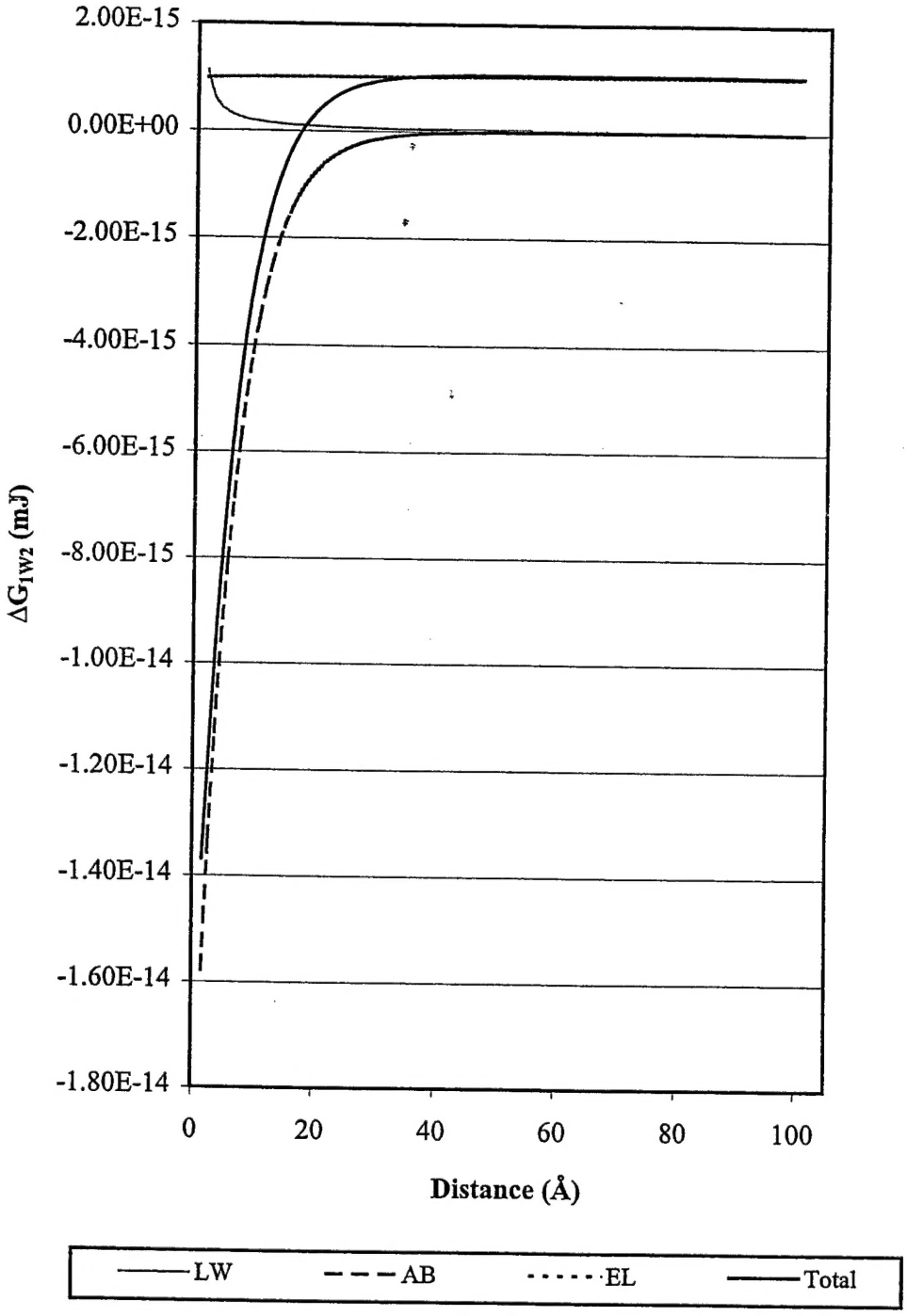

Figure A-8. Variation of Total Interaction Energy and Its Components with Distance Between ZVI and AER at Stationary State.

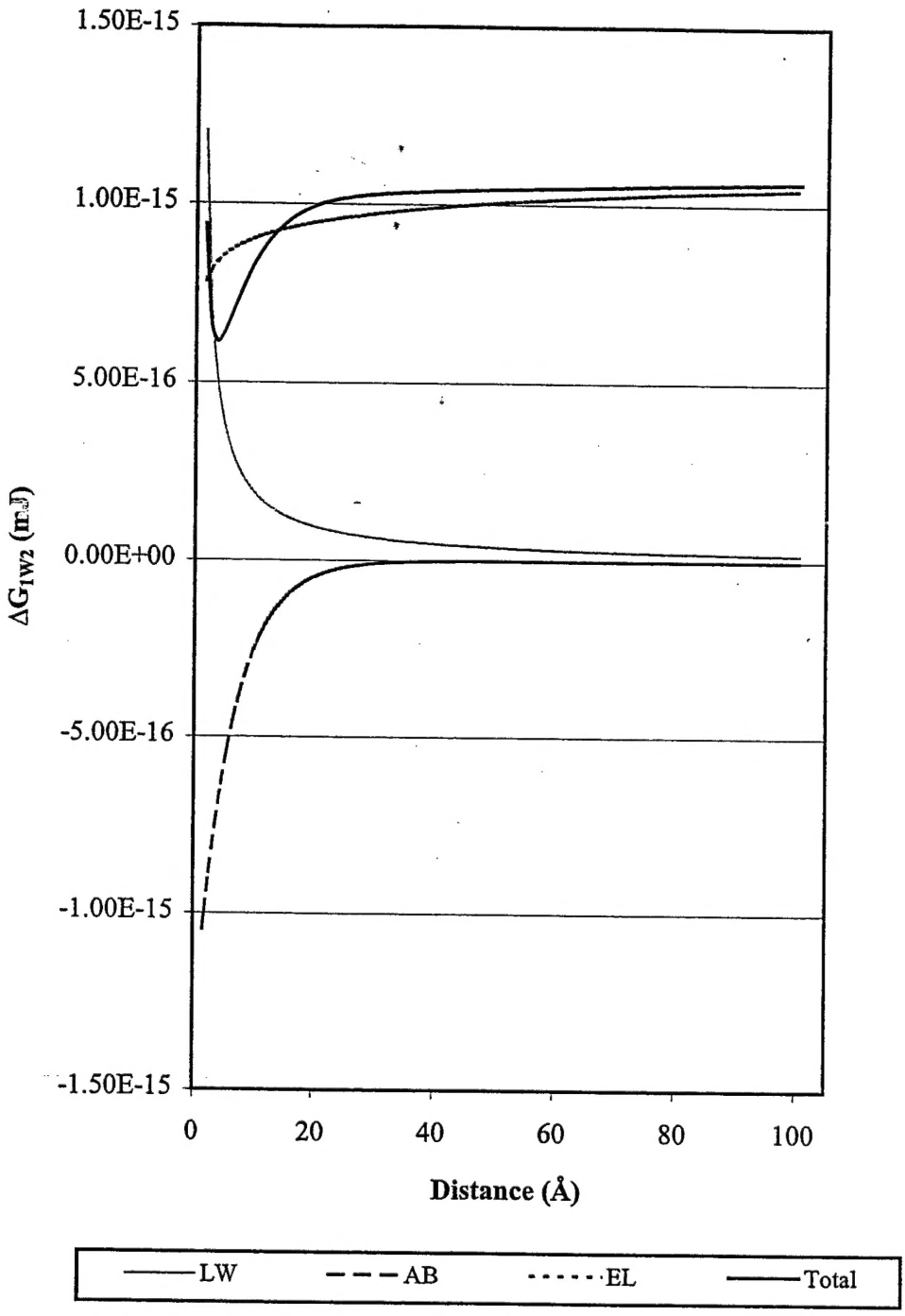

Figure A-9. Variation of Total Interaction Energy and Its Components with Distance Between ZVI and AER at Decay State.